Chapter 6

BEGOE(1+2)-s: Spectral Properties

6.1 Introduction

In the present chapter, our focus is on embedded ensembles for boson systems. As already emphasized in Chapter 1, unlike for fermion systems, there are only a few BEE investigations for finite interacting spinless boson systems [Ag-01, Ag-02, Ch-03, Ch-04]. Going beyond the embedded ensembles for spinless boson systems, our purpose in this chapter is to introduce and analyze spectral properties of embedded Gaussian orthogonal ensemble of random matrices for boson systems with spin degree of freedom [BEGOE(2)-s and also BEGOE(1+2)-s] and for Hamiltonians that conserve the total spin of the m-boson systems. Here the spin is, for example, as the F-spin in the proton-neutron interacting boson model (pnIBM) of atomic nuclei [Ca-05]. Just as the earlier BEE studies for spinless boson systems, a major motivation for the study undertaken in the present chapter is the possible applications of generalized BEEs to ultracold atoms. The BEGOE(1+2)-s with spin-$\frac{1}{2}$ bosons is a simple yet non-trivial extension of BEGOE(1+2). This ensemble is useful in obtaining several physical conclusions, like spin dependence of the order to chaos transition marker in level fluctuations, the spin of the gs, the spin ordering of excited states and pairing correlations in the gs region generated by random interactions, that explicitly require inclusion of spin degree of freedom. These are discussed in Secs. 6.3, 6.5 and 6.6.

It should be emphasized that the present chapter opens a new direction in defining and analyzing embedded ensembles for boson systems with symmetries. There are now many studies of spinor BEC using Hamiltonians conserving the total spin

with the bosons carrying $\mathbf{s} = 1$ (also higher) degree of freedom [Pe-10, Yi-07]. Also, there are several studies of the properties of a mixture of two species of atoms which correspond to pseudospin-$\frac{1}{2}$ bosons (i.e., two-component boson systems) with $m_{\mathbf{s}} = \pm\frac{1}{2}$ distinguishing the two species; see for example [Al-03, Sh-10]. However, the Hamiltonians appropriate for these studies do not conserve the total spin (as the system does not have true $\frac{1}{2}$-spins). BEE with good M_S are appropriate in understanding the statistical properties of these systems. These explorations are beyond the scope of the present thesis. Extensions of BEGOE(1+2)-s with $\mathbf{s} = \frac{1}{2}$ to boson ensembles with integer spin $\mathbf{s} = 1$ and to BEGOE(1+2)-M_S are briefly discussed in Appendix G for completeness. All the results presented in this chapter are reported in [Ma-11]. Now, we begin with the definition and construction of BEGOE(1+2)-s.

6.2 Definition and Construction of BEGOE(1+2)-s

Let us consider a system of m ($m > 2$) bosons distributed in Ω number of sp orbitals each with spin $\mathbf{s} = \frac{1}{2}$. Then the number of sp states is $N = 2\Omega$. The sp states are denoted by $|i, m_{\mathbf{s}} = \pm\frac{1}{2}\rangle$ with $i = 1, 2, \ldots, \Omega$ and the two-particle symmetric states are denoted by $|(ij)s, m_s\rangle$ with $s = 0$ or 1. It is important to note that for EGOE(1+2)-s, the embedding algebra is $U(2\Omega) \supset U(\Omega) \otimes SU(2)$ with $SU(2)$ generating spin; see Secs. 6.5 and 6.6 ahead. The dimensionalities of the two-particle spaces with $s = 0$ and $s = 1$ are $\Omega(\Omega - 1)/2$ and $\Omega(\Omega + 1)/2$, respectively. For one plus two-body Hamiltonians preserving m-particle spin S, the one-body Hamiltonian is $\widehat{h}(1) = \sum_{i=1}^{\Omega} \epsilon_i n_i$ where the orbitals i are doubly degenerate, n_i are number operators and ϵ_i are sp energies. The two-body Hamiltonian $\widehat{V}(2)$ preserving m-particle spin S is defined by the symmetrized two-body matrix elements $V^s_{ijkl} = \langle (kl)s, m_s | \widehat{V}(2) | (ij)s, m_s \rangle$ with $s = 0, 1$ and they are independent of the m_s quantum number; note that for $s = 0$, only $i \neq j$ and $k \neq l$ matrix elements exist. Thus $\widehat{V}(2) = \widehat{V}^{s=0}(2) + \widehat{V}^{s=1}(2)$ and the sum here is a direct sum. The BEGOE(2)-s ensemble for a given (m, S) system is generated by first defining the two parts of the two-body Hamiltonian to be independent GOE(1)'s in the two-particle spaces [one for $\widehat{V}^{s=0}(2)$ and other for $\widehat{V}^{s=1}(2)$]. Now the $V(2)$ ensemble defined by $\{\widehat{V}(2)\} = \{\widehat{V}^{s=0}(2)\} + \{\widehat{V}^{s=1}(2)\}$ is propagated to the (m, S)-spaces by using the geometry (direct product structure) of the m-particle spaces. By adding the

$\widehat{h}(1)$ part, the BEGOE(1+2)-s is defined by the operator

$$\{\widehat{H}\}_{\text{BEGOE(1+2)-s}} = \widehat{h}(1) + \lambda_0 \{\widehat{V}^{s=0}(2)\} + \lambda_1 \{\widehat{V}^{s=1}(2)\}. \tag{6.2.1}$$

Here λ_0 and λ_1 are the strengths of the $s = 0$ and $s = 1$ parts of $\widehat{V}(2)$, respectively. The mean-field one-body Hamiltonian $\widehat{h}(1)$ in Eq. (6.2.1) is defined by sp energies ϵ_i with average spacing Δ. As already mentioned in Chapter 2, we put $\Delta = 1$ so that λ_0 and λ_1 are in the units of Δ and choose $\epsilon_i = i + 1/i$. Thus BEGOE(1+2)-s is defined by the five parameters $(\Omega, m, S, \lambda_0, \lambda_1)$. The H matrix dimension $d_b(\Omega, m, S)$ for a given (m, S) is

$$d_b(\Omega, m, S) = \frac{(2S+1)}{(\Omega-1)} \binom{\Omega + m/2 + S - 1}{m/2 + S + 1} \binom{\Omega + m/2 - S - 2}{m/2 - S}, \tag{6.2.2}$$

and they satisfy the sum rule $\sum_S (2S + 1) \, d_b(\Omega, m, S) = \binom{N+m-1}{m}$. For example: (i) $d_b(4, 10, S) = 196, 540, 750, 770, 594$ and 286 for spins $S = 0 - 5$; (ii) $d_b(4, 11, S) = 504, 900, 1100, 1056, 780$ and 364 for $S = 1/2 - 11/2$; (iii) $d_b(5, 10, S) = 1176, 3150, 4125, 3850, 2574$ and 1001 for $S = 0 - 5$; (iv) $d_b(6, 12, S) = 13860, 37422, 50050, 49049, 36855, 20020$ and 6188 for $S = 0 - 6$; and (v) $d_b(6, 16, S) = 70785, 198198, 286650, 321048, 299880, 235620, 151164, 72675$ and 20349 for $S = 0 - 8$.

Given ϵ_i and V^s_{ijkl}, the many-particle Hamiltonian matrix for a given (m, S) can be constructed using the M_S representation (M_S is the S_z quantum number) and for spin projection the S^2 operator is used as it was done for fermion systems in Chapter 2. Alternatively, it is possible to construct the H matrix directly in a good S basis using angular-momentum algebra as it was done for fermion systems in [Tu-06]. We have employed the M_S representation for constructing the H matrices with $M_S = M_S^{min} = 0$ for even m and $M_S = M_S^{min} = \frac{1}{2}$ for odd m and they will contain states with all S values. The dimension of this basis space is $\mathscr{D}(\Omega, m, M_S^{min}) = \sum_S d_b(\Omega, m, S)$. For example, $\mathscr{D}(4, 10, 0) = 3136$, $\mathscr{D}(4, 11, \frac{1}{2}) = 4704$, $\mathscr{D}(5, 10, 0) = 15876$, $\mathscr{D}(6, 12, 0) = 213444$ and $\mathscr{D}(6, 16, 0) = 1656369$.

To construct the many-particle Hamiltonian matrix for a given (m, S), first the sp states $|i, m_s = \pm\frac{1}{2}\rangle$ are arranged in such a way that the first Ω states have $m_s = \frac{1}{2}$ and the remaining Ω states have $m_s = -\frac{1}{2}$ so that the sp states are $|r\rangle = |i = r, m_s = \frac{1}{2}\rangle$ for $r \le \Omega$ and $|r\rangle = |i = r - \Omega, m_s = -\frac{1}{2}\rangle$ for $r > \Omega$. Using the direct product structure

of the many-particle states, the m-particle configurations $\mathbf{m}$, in occupation number representation, are

$$\mathbf{m} = \left| \prod_{r=1}^{N=2\Omega} m_r \right\rangle = |m_1, m_2, \ldots, m_\Omega, m_{\Omega+1}, m_{\Omega+2}, \ldots, m_{2\Omega}\rangle, \qquad (6.2.3)$$

where $m_r \geq 0$ with $\sum_{r=1}^{N} m_r = m$ and $M_S = \frac{1}{2}\left[\sum_{r=1}^{\Omega} m_r - \sum_{r'=\Omega+1}^{2\Omega} m_{r'}\right]$. To proceed further, the (1+2)-body Hamiltonian defined by ϵ_i and $V_{ijkl}^{s=0,1}$ is converted into the $|i, m_\mathbf{s} = \pm\frac{1}{2}\rangle$ basis. Then the sp energies ϵ'_i with $i = 1, 2, \ldots, N$ are $\epsilon'_i = \epsilon'_{i+\Omega} = \epsilon_i$ for $i \leq \Omega$. Similarly, V_{ijkl}^s are changed to $V_{im_i, jm_j, km_k, lm_l} = \langle im_i, jm_j | V(2) | km_k, lm_l \rangle$ using,

$$V_{i\frac{1}{2}, j\frac{1}{2}, k\frac{1}{2}, l\frac{1}{2}} = V_{i-\frac{1}{2}, j-\frac{1}{2}, k-\frac{1}{2}, l-\frac{1}{2}} = V_{ijkl}^{s=1},$$

$$\qquad (6.2.4)$$

$$V_{i\frac{1}{2}, j-\frac{1}{2}, k\frac{1}{2}, l-\frac{1}{2}} = \frac{\sqrt{(1+\delta_{ij})(1+\delta_{kl})}}{2}\left[V_{ijkl}^{s=1} + V_{ijkl}^{s=0}\right],$$

with all the other matrix elements being zero except for the symmetries,

$$V_{im_i, jm_j, km_k, lm_l} = V_{km_k, lm_l, im_i, jm_j} = V_{jm_j, im_i, lm_l, km_k} = V_{im_i, jm_j, lm_l, km_k}. \qquad (6.2.5)$$

Using $(\epsilon'_r, V_{im_i, jm_j, km_k, lm_l})$'s, construction of the m-particle H matrix in the basis defined by Eq. (6.2.3) reduces to the problem of BEGOE(1+2) for spinless boson systems and hence Eq. (1.3.3) will give the formulas for the non-zero matrix elements; see Sec. 1.3 for details. Now diagonalizing the S^2 matrix in the basis defined by Eq. (6.2.3) will give the unitary transformation required to change the H matrix in M_S basis into good S basis. Following this method, we have numerically constructed BEGOE(1+2)-s in many examples and analyzed various spectral properties generated by this ensemble. In addition, we have also derived some analytical results as discussed ahead in Secs. 6.4 and 6.6. These results are also used to validate the BEGOE(1+2)-s numerical code we have developed. In addition, we have also verified the code by comparing the results with those [Ch-10] obtained by directly programming the operations that give Eq. (1.3.3). In this chapter, we deal with both BEGOE(2)-s and BEGOE(1+2)-s and the focus is on the dense limit defined by $m \to \infty$, $\Omega \to \infty$, $m/\Omega \to \infty$ and S is fixed. Now we will discuss these results.

6.3 Numerical Results for Eigenvalue Density and Level Fluctuations in the Dense Limit

We begin with the ensemble averaged fixed-(m, S) eigenvalue density $\rho^{m,S}(E)$, the one-point function for eigenvalues. First we present the results for BEGOE(2)-s ensemble defined by $\widehat{h}(1) = 0$ in Eq. (6.2.1) and then the Hamiltonian operator is,

$$\{\widehat{H}\}_{\text{BEGOE(2)-s}} = \lambda_0 \{\widehat{V}^{s=0}(2)\} + \lambda_1 \{\widehat{V}^{s=1}(2)\}. \tag{6.3.1}$$

We have considered a 500 member BEGOE(2)-s ensemble with $\Omega = 4$ and $m = 10$ and similarly a 100 member ensemble with $\Omega = 4$ and $m = 11$. Here and in all other numerical results presented in the present chapter, we use $\lambda_0 = \lambda_1 = \lambda$. In the construction of the ensemble averaged eigenvalue densities, the spectra of each member of the ensemble is first zero centered and scaled to unit width (therefore the densities are independent of the λ parameter). The eigenvalues are then denoted by $\widehat{E}$. Given the fixed-(m, S) energy centroids $E_c(m, S)$ and spectral widths $\sigma(m, S)$, $\widehat{E} = [E - E_c(m, S)]/\sigma(m, S)$. Then the histograms for the density are generated by combining the eigenvalues $\widehat{E}$ from all the members of the ensemble. Results are shown in Fig. 6.1 for a few selected S values. The calculations have been carried out for all S values (the results for other S values are close to those given in the figure) and also for many other BEGOE(2)-s examples. It is clearly seen that the eigenvalue densities are close to Gaussian (denoted by $\mathcal{G}$ below) with the ensemble averaged skewness (γ_1) and excess (γ_2) being very small; $|\gamma_1| \sim 0$, $|\gamma_2| \sim 0.1 - 0.27$. The agreements with Edgeworth (ED) corrected Gaussians are excellent. The ED form that includes γ_1 and γ_2 corrections is given by ρ_{ED} in Eq. (2.3.2).

For the analysis of level fluctuations (equivalent to studying the two-point function for the eigenvalues), each spectrum in the ensemble is unfolded using a sixth order polynomial correction to the Gaussian and then the smoothed density is $\overline{\eta(\widehat{E})} = \eta_{\mathcal{G}}(\widehat{E})\{1 + \sum_{\zeta \geq 3}^{\zeta_0}(\zeta!)^{-1} S_\zeta He_\zeta(\widehat{E})\}$ with $\zeta_0 = 6$ [Le-08, Pa-00]. The parameters S_ζ are determined by minimizing $\Delta^2 = \sum_{i=1}^{d_b(\Omega, m, S)} [F(E_i) - \overline{F(E)}]^2$. The distribution function $F(E) = \int_{-\infty}^{E} \eta(x) dx$ and similarly $\overline{F(E)}$ is defined. We require that the continuous function $\overline{F(E)}$ passes through the mid-points of the jumps in the discrete $F(E)$ and
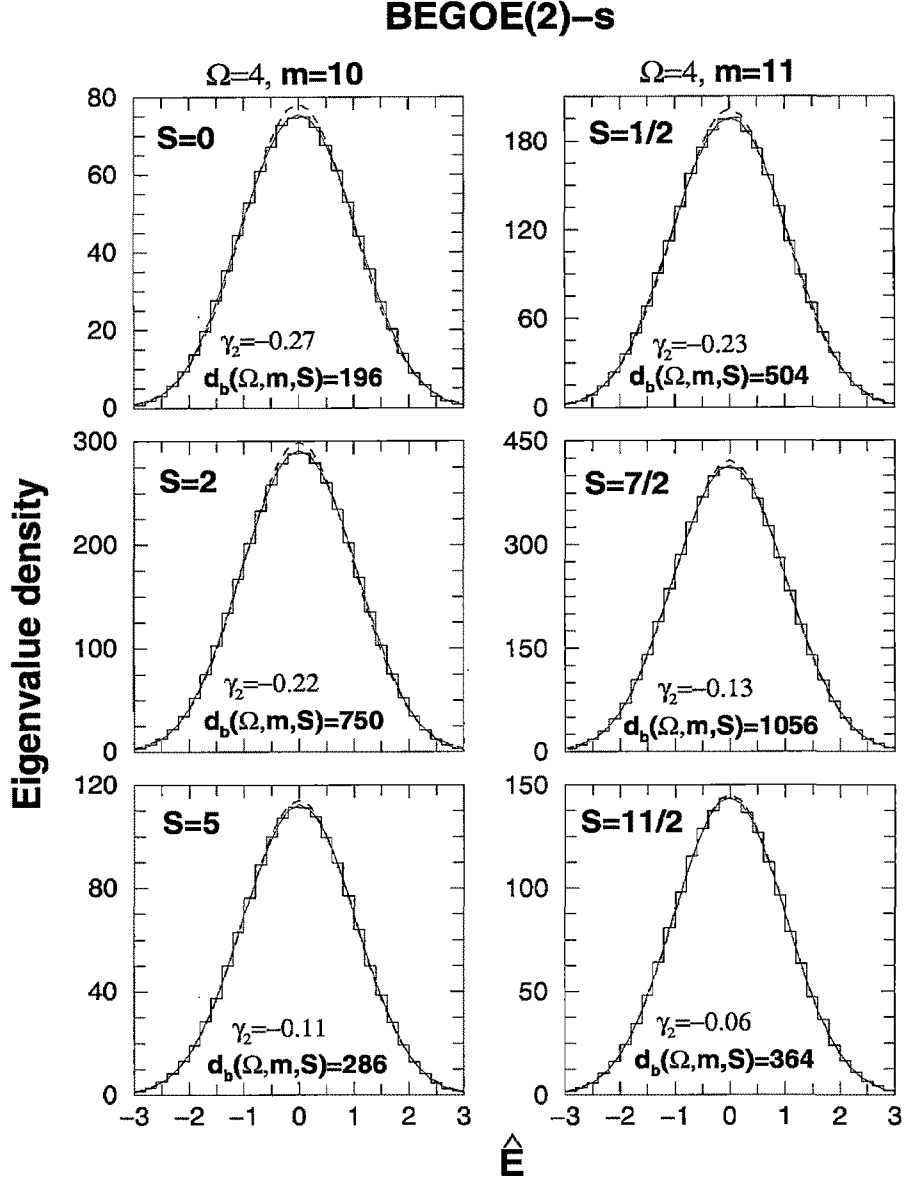
BEGOE(2)-s

Figure 6.1: Ensemble averaged eigenvalue density $\rho^{m,S}(\widehat{E})$ vs $\widehat{E}$ for BEGOE(2)-s ensembles with $\Omega = 4$, $m = 10$ and $\Omega = 4$, $m = 11$. In the figure, histograms constructed with a bin size 0.2 are BEGOE(2)-s results and they are compared with Gaussian (dashed red) and Edgeworth (ED) corrected Gaussian (solid green) forms. The ensemble averaged values of the excess parameter (γ_2) are also shown in the figure. In the plots, the area under the curves is normalized to the dimensions $d_b(\Omega, m, S)$. See text for further details.

therefore, $F(E_i) = (i - 1/2)$. The ensemble averaged Δ_{RMS} is ~ 3 for $\zeta_0 = 3$, ~ 1 for $\zeta_0 = 4$ and ~ 0.8 for $\zeta_0 = 6$ with some variation with respect to S. As $\Delta_{RMS} \sim 0.88$ for GOE, this implies GOE fluctuations set in when we add 6th order corrections to the asymptotic Gaussian density. Using the unfolded energy levels of all the mem-

bers of the BEGOE(2)-s ensemble, the nearest neighbor spacing distribution (NNSD) that gives information about level repulsion and the Dyson-Mehta $\overline{\Delta_3}(L)$ statistic that gives information about spectral rigidity are studied. Results for the same systems used in Fig. 6.1 are shown in Fig. 6.2 with $S = 2$ and 5 for $m = 10$ and $S = 7/2$ and $11/2$ for $m = 11$ (for other spins, the results are similar). In the calculations, middle 80% of the eigenvalues from each member are employed. It is clearly seen from the figures that the NNSD are close to GOE (Wigner) form and the widths of the NNSD are ~ 0.288 (GOE value is ~ 0.272). The $\overline{\Delta_3}(L)$ values show some departures from GOE for $L \gtrsim 30$ for $S = S_{max}$ and this could be because the matrix dimensions are small for $S = S_{max}$ in our examples (also the systems considered are not strictly in the dense limit and numerical examples with much larger m and Ω with $m >> \Omega$ are currently not feasible). It is useful to add that $S = S_{max}$ states are important for boson systems with random interactions as discussed in Secs. 6.4-6.6 ahead. In conclusion, sixth order unfolding removes essentially all the secular behavior and then the fluctuations follow closely GOE. This is similar to the result known before for spinless boson systems [Le-08, Ch-03].

Going beyond BEGOE(2)-s, calculations are also carried out for BEGOE(1+2)-s systems using Eq. (6.2.1) with $\lambda_0 = \lambda_1 = \lambda$. We have verified the Gaussian behavior for the eigenvalue density for BEGOE(1+2)-s; an example is shown in Fig. 6.3(a). This result is essentially independent of λ. In addition, we have also verified that BEGOE(1+2)-s also generates level fluctuations close to GOE for $\lambda \gtrsim 0.1$ for $\Omega = 4$ and $m = 10$, 11 systems; Figs. 6.3(b) and 6.3(c) show the results for $\lambda = 0.1$ for $\Omega = 4$, $m = 11$, $S = 7/2$ system. Going beyond this, in Fig. 6.4, we show the NNSD results, for a 100 member BEGOE(1+2)-s ensemble with $\Omega = 4$, $m = 10$ and total spins $S = 0$, 2 and 5, by varying λ from 0.01 to 0.1 to demonstrate that as λ increases from zero, there is generically Poisson to GOE transition. A similar study is reported in Chapter 2 for fermion systems. As discussed there, for very small λ, the NNSD will be Poisson (as we use sp energies to be $\epsilon_i = i + 1/i$, the $\lambda = 0$ limit will not give strictly a Poisson). Moreover, as discussed in detail in Chapter 2, the variance of the NNSD can be written in terms of a parameter Λ (Λ is a parameter in a 2×2 random matrix model that generates Poisson to GOE transition) with $\Lambda = 0$ giving Poisson, $\Lambda \gtrsim 1$ GOE and $\Lambda = 0.3$ the transition point λ_c that marks the onset of GOE fluctuations. We show in
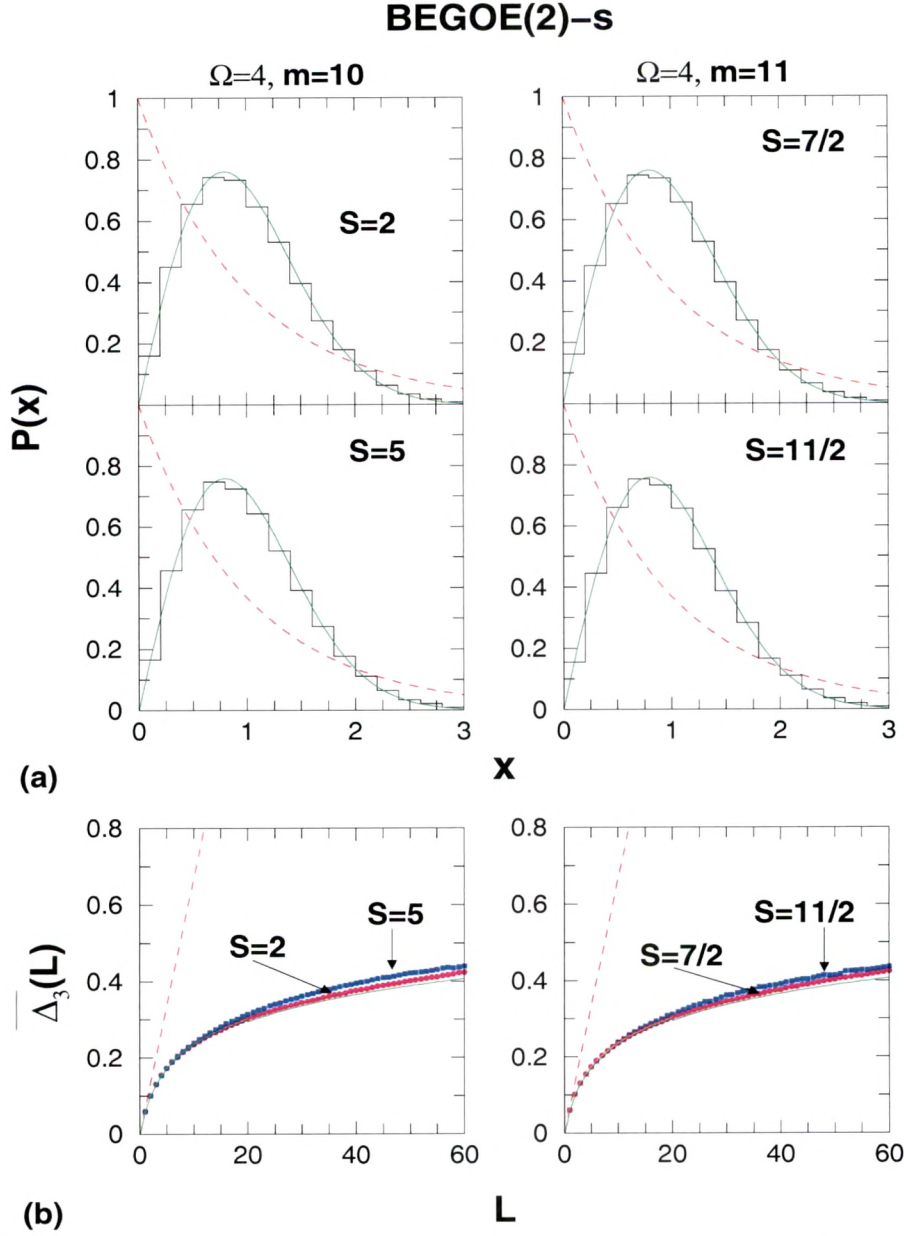
BEGOE(2)–s

Figure 6.2: (a) Ensemble averaged nearest neighbor spacing distribution (NNSD) and (b) Dyson-Mehta statistic $\overline{\Delta_3}(L)$ vs L for $L \leq 60$. Results are for the same systems considered in Fig. 6.1; first column gives the results for ($\Omega = 4$, $m = 10$) and the second column for ($\Omega = 4$, $m = 11$) systems. The NNSD histograms from BEGOE(2)-**s** are compared with Poisson (dashed red) and GOE (Wigner) forms (solid green) and similarly the $\overline{\Delta_3}(L)$ results. In the NNSD graphs, the bin-size is 0.2 and x is the nearest neighbor spacing in the units of local mean spacing. See text and Fig. 6.1 for further details.
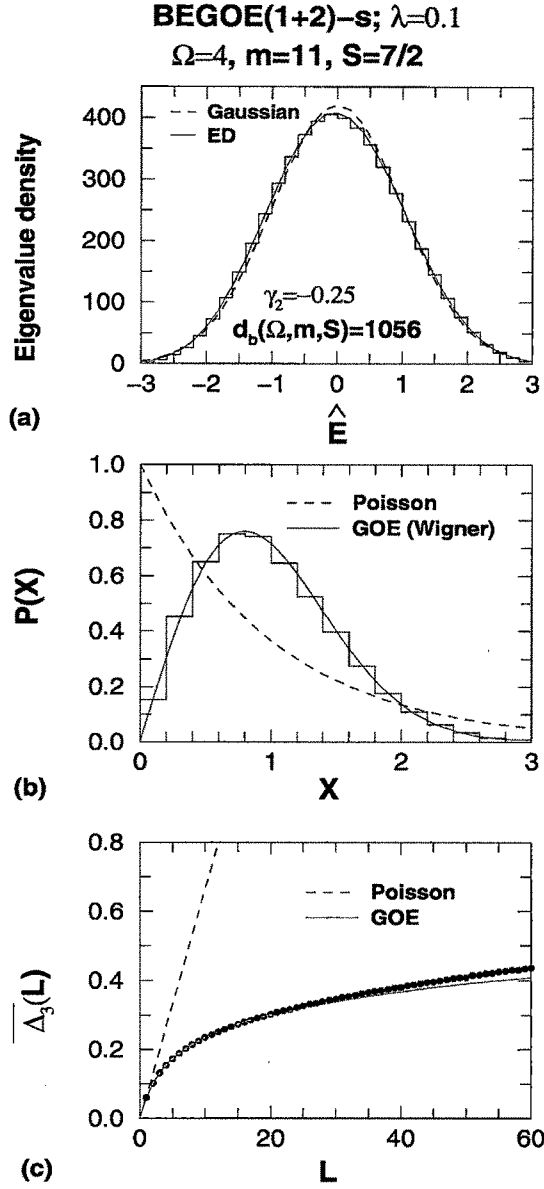
BEGOE(1+2)-s; λ=0.1
Ω=4, m=11, S=7/2

Figure 6.3: (a) Ensemble averaged eigenvalue density $\rho^{m,S}(\widehat{E})$, (b) NNSD and (c) $\overline{\Delta_3}(L)$ vs. L for a 100 member BEGOE(1+2)-s ensemble for $\Omega = 4$, $m = 11$ and $S = 7/2$ system with $\lambda_0 = \lambda_1 = \lambda = 0.1$ in Eq. (6.2.1). For all other details, see text and Figs. 6.1 and 6.2.

Fig. 6.4, for each λ, the deduced value of Λ from the variance of the NNSD (Fig. 6.2 gives the results for $\lambda \rightarrow \infty$). As seen from the Fig. 6.4, λ_c = 0.039, 0.0315, 0.0275 for $S = 0, 2$, and 5, respectively. Thus λ_c decreases with increasing spin S and this is opposite to the situation for fermion systems. For a fixed Ω value, as discussed in Chapter 2, the λ_c is inversely proportional to K, where K is the number of many-particle states [defined by $h(1)$] that are directly coupled by the two-body interaction. For fermion
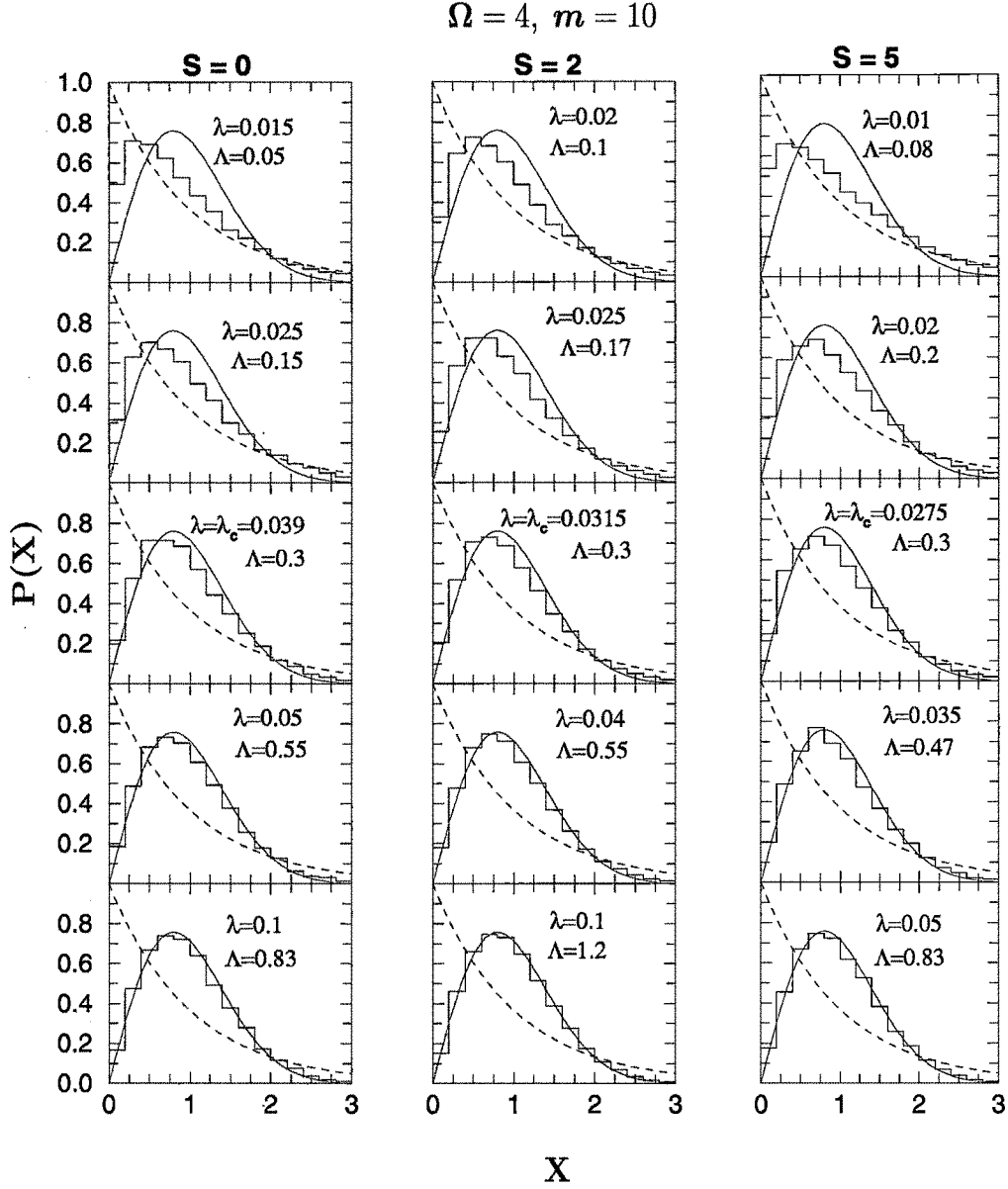
$$\Omega = 4, \ m = 10$$

Figure 6.4: NNSD for a 100 member BEGOE(1+2)-s ensemble with $\Omega = 4$, $m = 10$ and spins $S = 0$, 2 and 5. Calculated NNSD are compared to the Poisson (red dashed) and Wigner (GOE) (green solid) forms. Values of the interaction strength λ and the transition parameter Λ are given in the figure. The values of Λ are deduced as discussed in Chapter 2. The chaos marker λ_c corresponds to $\Lambda = 0.3$ and its values, as shown in the figure, are 0.039, 0.0315, 0.0275 for $S = 0$, 2, and 5, respectively. Bin-size for the histograms is 0.2.

systems, K is proportional to the variance propagator but not for boson systems as discussed in [Ch-03]. At present, for BEGOE(1+2)-s we don't have a formula for K. However, if we use the variance propagator $Q(\Omega, m, S)$ for the boson systems [see Eq. (6.4.7) and Fig. 6.5 ahead], then qualitatively we understand the decrease in λ_c with

increasing spin.

Finally, it is well-known that the Gaussian form for the eigenvalue density is generic for embedded ensembles of spinless boson (also fermion) systems; see Chapter 1. In addition, ensemble averaged fixed-(m, S) eigenvalue densities for the fermion EGOE(1+2)-s are shown to take Gaussian form; see Chapter 2. Hence, from the results shown in Figs. 6.1 and 6.3(a), it is plausible to conclude that the Gaussian form is generic for BEE (also EE) with good quantum numbers. With the eigenvalue density being close to Gaussian, it is useful to derive formulas for the energy centroids and ensemble averaged spectral variances. These in turn, as already discussed in Chapter 4, will also allow us to study the lowest two moments of the two-point function. From now on, we will drop the "hat" over the operators H, $h(1)$ and $V(2)$ when there is no confusion.

6.4 Energy Centroids, Spectral Variances and Ensemble Averaged Spectral Variances and Covariances

6.4.1 Propagation formulas for energy centroids and spectral variances

Given a general (1+2)-body Hamiltonian $H = h(1) + V(2)$, which is a typical member of BEGOE(1+2)-s, the energy centroids will be polynomials in the number operator and the S^2 operator. As H is of maximum body rank 2, the polynomial form for the energy centroids is $\langle H \rangle^{m,S} = E_c(m, S) = a_0 + a_1 m + a_2 m^2 + a_3 S(S + 1)$. Solving for the a's in terms of the centroids in one and two-particle spaces, the propagation formula for the energy centroids is,

$$\langle H \rangle^{m,S} = E_c(m, S) = \left[\langle h(1) \rangle^{1,\frac{1}{2}} \right] m + \lambda_0 \left\langle \left\langle V^{s=0}(2) \right\rangle \right\rangle^{2,0} \frac{P^0(m, S)}{4\Omega(\Omega - 1)}$$

$$+ \lambda_1 \left\langle \left\langle V^{s=1}(2) \right\rangle \right\rangle^{2,1} \frac{P^1(m, S)}{4\Omega(\Omega + 1)} ;$$

$$P^0(m, S) = [m(m + 2) - 4S(S + 1)] , \quad P^1(m, S) = [3m(m - 2) + 4S(S + 1)] ,$$

$$\langle h(1) \rangle^{1,\frac{1}{2}} = \bar{\epsilon} = \Omega^{-1} \sum_{i=1}^{\Omega} \epsilon_i ,$$

(6.4.1)

169

$$\langle\langle V^{s=0}(2)\rangle\rangle^{2,0} = \sum_{i<j} V^{s=0}_{ijij}, \quad \langle\langle V^{s=1}(2)\rangle\rangle^{2,1} = \sum_{i\leq j} V^{s=1}_{ijij}.$$

For the energy centroid of a two-body Hamiltonian [member of a BEGOE(2)-s], the $h(1)$ part in Eq. (6.4.1) will be absent.

Just as for the energy centroids, polynomial form for the spectral variances

$$\sigma^2_{H=h(1)+V(2)}(m,S) = \langle H^2\rangle^{m,S} - [E_c(m,S)]^2$$

is $\sum_{p=0}^{4} a_p m^p + \sum_{q=0}^{2} b_q m^q S(S+1) + c_0 [S(S+1)]^2$. It is well-known that the propagation formulas for fermion systems will give the formulas for the corresponding boson systems by applying $\Omega \to -\Omega$ transformation [Ko-79a,Ko-80,Ko-81,Cv-82,Ko-05]. Applying this transformation to the propagation equation for the spectral variances for fermion systems with spin given by Eq. (B2), we obtain the propagation equation for $\sigma^2_{H=h(1)+V(2)}(m,S)$ in terms of inputs that contain the sp energies ϵ_i defining $h(1)$ and the two-particle matrix elements V^s_{ijkl}. The final result is,

$$\sigma^2_{H=h(1)+V(2)}(m,S) = \langle H^2\rangle^{m,S} - [E_c(m,S)]^2$$

$$= \frac{(\Omega-2)mm^\star + 2\Omega\langle S^2\rangle}{(\Omega-1)\Omega(\Omega+1)} \sum_i \tilde{\epsilon}_i^2$$

$$+ \frac{m^\star P^0(m,S)}{2(\Omega-1)\Omega(\Omega+1)} \sum_i \tilde{\epsilon}_i \lambda_{i,i}(0)$$

$$+ \frac{(\Omega-2)m^\star P^1(m,S) + 8\Omega(m-1)\langle S^2\rangle}{2(\Omega-1)\Omega(\Omega+1)(\Omega+2)} \sum_i \tilde{\epsilon}_i \lambda_{i,i}(1) \qquad (6.4.2)$$

$$+ P^{v=1,s=0}(m,S) \sum_{i,j} \lambda_{i,j}^2(0) + P^{v=1,s=1}(m,S) \sum_{i,j} \lambda_{i,j}^2(1)$$

$$+ \frac{P^2(m,S)P^0(m,S)}{4(\Omega-1)\Omega(\Omega+1)(\Omega+2)} \sum_{i,j} \lambda_{i,j}(0)\lambda_{i,j}(1)$$

$$+ P^{v=2,s=0}(m,S) \langle (V^{v=2,s=0})^2\rangle^{2,0} + P^{v=2,s=1}(m,S) \langle (V^{v=2,s=1})^2\rangle^{2,1}.$$

The propagators $P^{\nu,s}$'s, which are used later, are

$$P^{\nu=1,s=0}(m,S) = \frac{[(m+2)m^\star/2 - \langle S^2 \rangle] P^0(m,S)}{8(\Omega-2)(\Omega-1)\Omega(\Omega+1)},$$

$$P^{\nu=1,s=1}(m,S) = \frac{8\Omega(m-1)(\Omega+2m-4)\langle S^2 \rangle + (\Omega-2)P^2(m,S)P^1(m,S)}{8(\Omega-1)\Omega(\Omega+1)(\Omega+2)^2},$$

$$P^{\nu=2,s=0}(m,S) = [m^\star(m^\star-1) - \langle S^2 \rangle] P^0(m,S)/[8\Omega(\Omega+1)], \tag{6.4.3}$$

$$P^{\nu=2,s=1}(m,S) = \Big\{[\langle S^2 \rangle]^2 (3\Omega^2 + 7\Omega + 6)/2 + 3m(m-2)m^\star(m^\star+1)$$
$$\times (\Omega-1)(\Omega-2)/8 + [\langle S^2 \rangle/2] [(5\Omega+3)(\Omega-2)mm^\star + \Omega(\Omega-1)(\Omega+1)$$
$$\times(\Omega-6)]\Big\}/[(\Omega-1)\Omega(\Omega+2)(\Omega+3)];$$
$$P^2(m,S) = 3(m-2)m^\star/2 + \langle S^2 \rangle, \quad m^\star = \Omega + m/2, \quad \langle S^2 \rangle = S(S+1).$$

The inputs in Eq. (6.4.2) are given by,

$$\tilde{\epsilon}_i = \epsilon_i - \bar{\epsilon},$$

$$\lambda_{i,i}(s) = \sum_j V^s_{ijij}(1+\delta_{ij}) - (\Omega)^{-1} \sum_{k,l} V^s_{klkl}(1+\delta_{kl}),$$

$$\lambda_{i,j}(s) = \sum_k \sqrt{(1+\delta_{ki})(1+\delta_{kj})}\, V^s_{kikj} \quad \text{for } i \neq j,$$

$$\tag{6.4.4}$$

$$V^{\nu=2,s}_{ijij} = V^s_{ijij} - [\langle V(2) \rangle^{2,s} + (\lambda_{i,i}(s) + \lambda_{j,j}(s))(\Omega-2(-1)^s)^{-1}],$$

$$V^{\nu=2,s}_{kikj} = V^s_{kikj} - (\Omega-2(-1)^s)^{-1}\sqrt{(1+\delta_{ki})(1+\delta_{kj})}\,\lambda^s_{i,j} \quad \text{for } i \neq j,$$

$$V^{\nu=2,s}_{ijkl} = V^s_{ijkl} \quad \text{for all other cases}.$$

Eqs. (6.4.1) and (6.4.2) can be applied to individual members of the BEGOE(1+2) ensemble. On the other hand, it is possible to use these to obtain ensemble averaged spectral variances and ensemble averaged covariances in energy centroids just as it was done before for fermion systems; see Chapter 2 for details. Now we will consider these.

171

6.4.2 Ensemble averaged spectral variances for BEGOE(2)-s

In the present subsection, we restrict to $H = V(2)$ i.e., BEGOE(2)-s and consider BEGOE(1+2)-s at the end.

For the ensemble averaged spectral variances generated by H, only the fourth, fifth, seventh and eighth terms in Eq. (6.4.2) will contribute. Evaluating the ensemble averages of the inputs in these four terms, we obtain,

$$\overline{\sum_{i,j} \lambda_{i,j}^2 (0)} = \lambda_0^2 (\Omega - 1)(\Omega - 2)(\Omega + 2) ,$$

$$\overline{\sum_{i,j} \lambda_{i,j}^2 (1)} = \lambda_1^2 (\Omega - 1)(\Omega + 2)^2 ,$$

(6.4.5)

$$\overline{\left\langle \left(H^{v=2,s=0} \right)^2 \right\rangle^{2,0}} = \lambda_0^2 \frac{(\Omega - 3)(\Omega^2 + \Omega + 2)}{2(\Omega - 1)} ,$$

$$\overline{\left\langle \left(H^{v=2,s=1} \right)^2 \right\rangle^{2,1}} = \lambda_1^2 \frac{(\Omega - 1)(\Omega + 2)}{2} .$$

Note that these inputs follow from the results for EGOE(2)-s for fermions given in Chapter 2 by interchanging $s = 0$ with $s = 1$. Now the final expression for the ensemble averaged variances is

$$\overline{\sigma_H^2 (m, S)} = \sum_{s=0,1} \lambda_s^2 (\Omega - 1)(\Omega - (-1)^s 2)(\Omega + 2) \, P^{v=1,s}(m, S)$$

$$+ \lambda_0^2 \frac{(\Omega - 3)(\Omega^2 + \Omega + 2)}{2(\Omega - 1)} \, P^{v=2,s=0}(m, S) \qquad (6.4.6)$$

$$+ \lambda_1^2 \frac{(\Omega - 1)(\Omega + 2)}{2} \, P^{v=2,s=1}(m, S) .$$

In most of the numerical calculations, we employ $\lambda_0 = \lambda_1 = \lambda$ and then $\overline{\sigma_H^2 (m, S)}$ takes the form,

$$\overline{\sigma_H^2 (m, S)} \stackrel{\lambda_0 = \lambda_1 = \lambda}{\longrightarrow} \lambda^2 Q(\Omega, m, S) . \qquad (6.4.7)$$

Expression for the variance propagator $Q(\Omega, m, S)$ follows easily from Eqs. (6.4.1), (6.4.3) and (6.4.6). In Fig. 6.5, we show a plot of $Q(\Omega, m, S)/Q(\Omega, m, S_{max})$ vs S/S_{max}
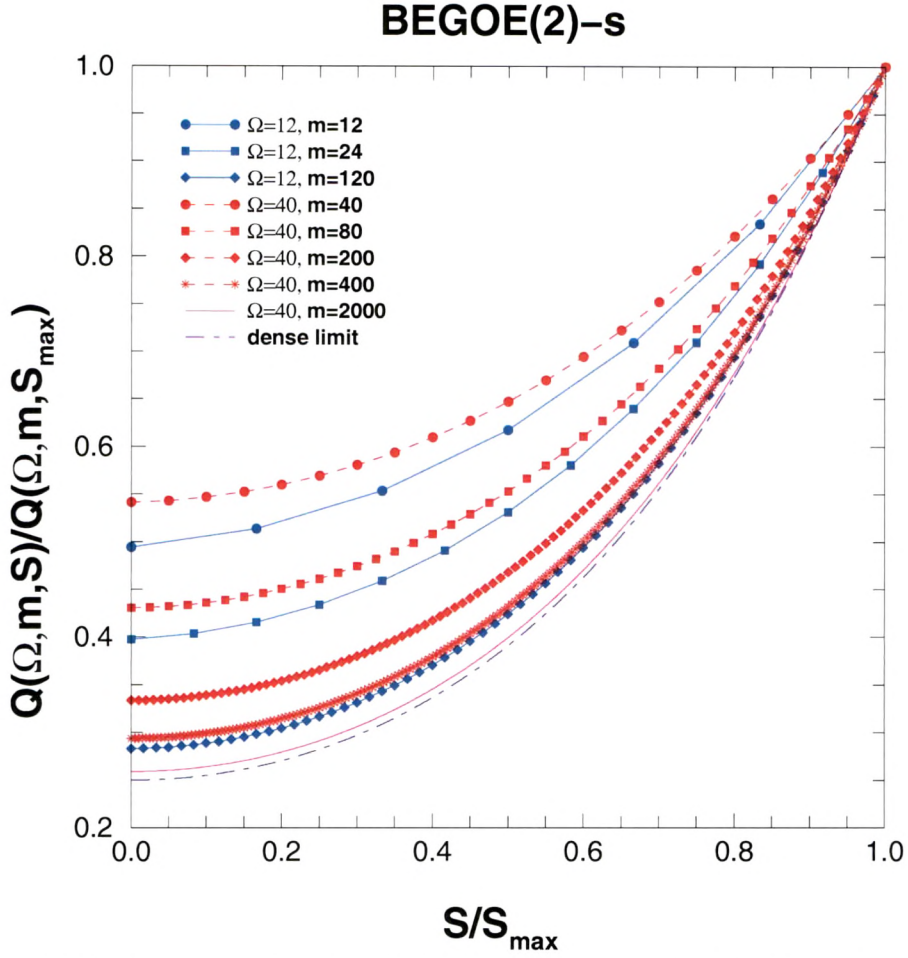
BEGOE(2)–s

Figure 6.5: BEGOE(2)-**s** variance propagator Q(Ω,m,S)/Q(Ω, m,S_{max}) vs S/S_{max} for various values of Ω and m. Formula for Q(Ω,m,S) follows from Eqs. (6.4.3), (6.4.6) and (6.4.7). Note that the results in the figure are for $\lambda_0 = \lambda_1 = \lambda$ in Eq. (6.3.1) and therefore independent of λ. Dense limit (dot-dashed) curve corresponds to the result given by Eq. (6.4.10) with $m = 2000$.

for various Ω and m values. It is clearly seen that the propagator value increases as spin increases and this is just opposite to the result for fermion systems (see Fig. 2.2). An important consequence of this is BEGOE(2)-**s** gives ground states with $S = S_{max}$ [for fermion EGOE(2)-**s**, the ground states with random interactions have $S = 0$; see Figs. 2.2 and 3.5]. This result follows from Eq. (4.6.1) with f_m replaced by S.

Before proceeding further, let us remark that for the BEGOE(1+2)-**s** Hamiltonian $\{H\} = h(1) + \{V(2)\}$, assuming that $h(1)$ is fixed, we have $\overline{\sigma_H^2} = \sigma_{h(1)}^2 + \overline{\sigma_{V(2)}^2}$. The first term $\sigma_{h(1)}^2$ is given by the first term of Eq. (6.4.2) and the second term is given by Eq. (6.4.6). In the situation $h(1)$ is represented by an ensemble independent of $\{V(2)\}$, we have to replace $\sigma_{h(1)}^2$ by $\overline{\sigma_{h(1)}^2}$ in $\overline{\sigma_H^2}$.

173

6.4.3 Ensemble averaged covariances in energy centroids and spectral variances for BEGOE(2)-s

Normalized covariances in energy centroids Σ_{11} and spectral variances Σ_{22} are defined by Eq. (4.4.8) with $\Gamma = S$. These define the lowest two moments of the two-point function, $S^{m,S:m',S'}(E,W)$; see Eq. (4.4.6). For $(m,S) = (m',S')$ they will give information about fluctuations and in particular about level motion in the ensemble [Pa-00]. For $(m,S) \neq (m',S')$, the covariances (cross-correlations) are non-zero for BEGOE while they will be zero for independent GOE representation for the m boson Hamiltonian matrices with different m or S. Note that the Ω value has to be same for both (m,S) and (m',S') systems so that the Hamiltonian in two-particle spaces remains same. Now we will discuss analytical and numerical results for Σ_{11} and numerical results for Σ_{22} for large values of (Ω, m) and they are obtained using the results in Secs. 6.4.1 and 6.4.2.

Trivially, the ensemble average of the energy centroids $E_c(m,S)$ will be zero [note that H is two-body for BEGOE(2)-s]; i.e., $\overline{\langle H \rangle^{m,S}} = 0$. However the covariances in the energy centroids of H are non-zero and Eq. (6.4.1) gives,

$$
\overline{\langle H \rangle^{m,S} \langle H \rangle^{m',S'}} =
\frac{\lambda_0^2}{16\Omega(\Omega-1)} P^0(m,S)\, P^0(m',S') + \frac{\lambda_1^2}{16\Omega(\Omega+1)} P^1(m,S)\, P^1(m',S') .
\tag{6.4.8}
$$

Equations (6.4.6), (6.4.7) and (6.4.8) allow us to calculate Σ_{11} for any (Ω, m, S). For $m = m'$ and $S = S'$, the $[\Sigma_{11}]^{1/2}$ gives the width ΔE_c of the fluctuations in the energy centroids. In the numerical calculations, we use $\lambda_0 = \lambda_1 = \lambda$ and therefore, Σ_{11} and Σ_{22} are independent of λ. Figure 6.6 gives some numerical results for ΔE_c and it is seen that : (i) for $m \gg \Omega$, the ΔE_c is $\sim 20\%$ for $S = 0$ and it goes down to $\sim 15\%$ for $S = S_{max} = m/2$ for $\Omega = 12$; (ii) going from $\Omega = 12$ to 40, ΔE_c decreases to $\sim 2-7\%$; (iii) for fixed (m,Ω), there is decrease in ΔE_c with increasing S value; (iv) for fixed (m,S) and very large m value, there is a sharp decrease in ΔE_c with increasing Ω up to $\Omega \sim 20$ and then it slowly converges to zero. It is possible to understand these results and the results for cross-correlations $[\Sigma_{11}(m,S:m',S')]^{1/2}$, with $(m,S) \neq (m',S')$ as shown in Fig. 6.7, using the asymptotic structure of $Q(\Omega, m, S)$.
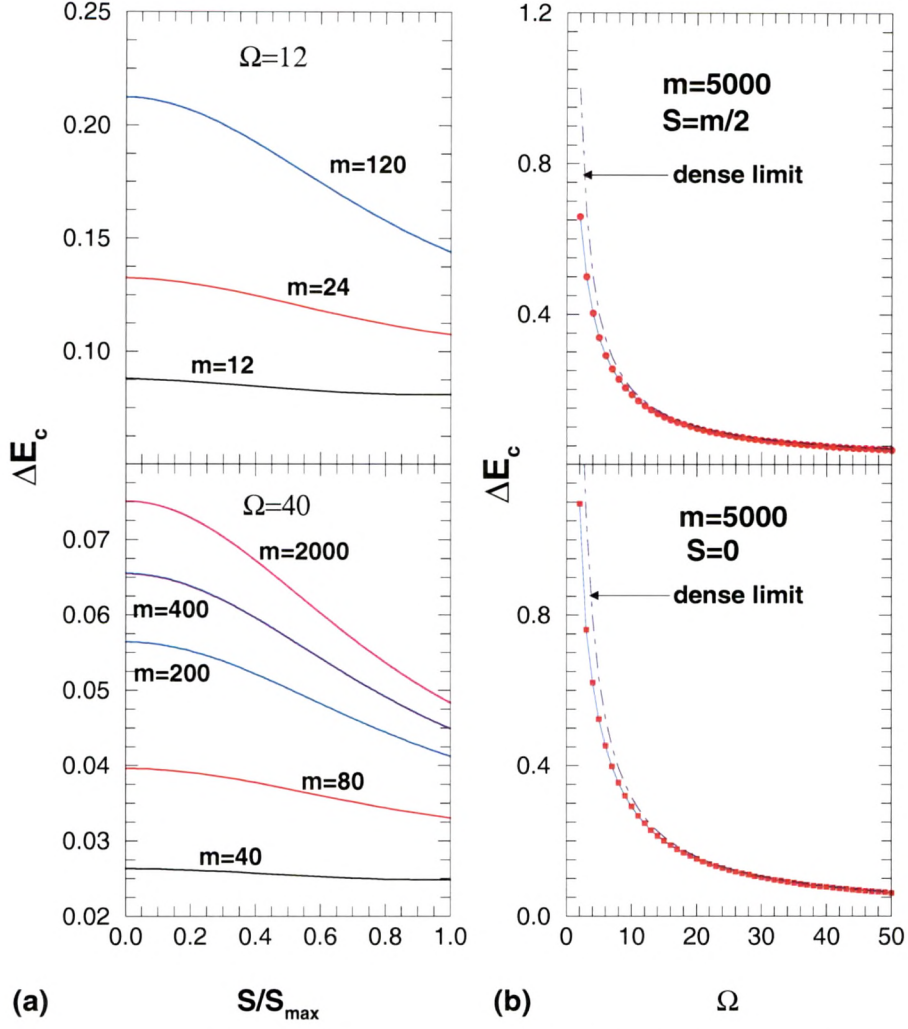
BEGOE(2)–s

Figure 6.6: (a) Self-correlations $\Sigma_{11}^{1/2}$ in energy centroids, giving width ΔE_c of the fluctuations in energy centroids scaled to the spectrum width, as a function of spin S for different values of m and Ω. (b) Self-correlations as a function of Ω for 5000 bosons with minimum spin ($S = 0$) and maximum spin ($S = 2500$). Dense limit (dot-dashed) curves for $S = 0$ and $S = m/2$ in (b) correspond to the results given by Eq. (6.4.12). See text for details.

Let us consider the dense limit defined by $m \to \infty$, $\Omega \to \infty$ and $m/\Omega \to \infty$. Firstly the $P^{\nu,s}(m, S)$ in Eq. (6.4.3) take the simpler forms, with $\mathscr{S}^2 = S(S+1)$,

$$P^{\nu=1,s=0} = \frac{\left(m^2 - 4\mathscr{S}^2\right)^2}{32\Omega^4} \,, \quad P^{\nu=1,s=1} = \frac{64m^2\mathscr{S}^2\left(3m^2 + 4\mathscr{S}^2\right)^2}{32\Omega^4} \,,$$

$$P^{\nu=2,s=0} = \frac{\left(m^2 - 4\mathscr{S}^2\right)^2}{32\Omega^2} \,, \quad P^{\nu=2,s=1} = \frac{3m^4 + 40m^2\mathscr{S}^2 + 48(\mathscr{S}^2)^2}{32\Omega^2} \,.$$
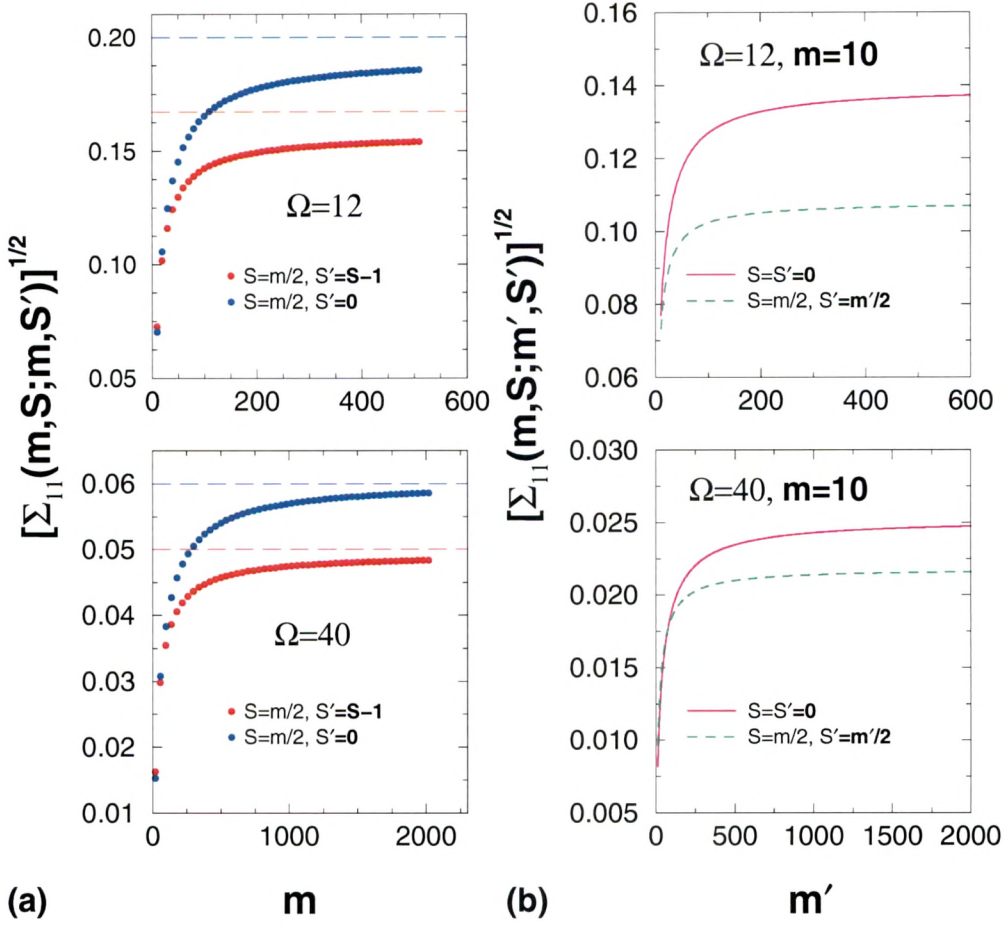
$$(6.4.9)$$

175

BEGOE(2)–s

Figure 6.7: Cross-correlations $\Sigma_{11}^{1/2}$ in energy centroids for various BEGOE(2)-**s** systems. (a) $\Sigma_{11}^{1/2}$ vs m with $m = m'$ but different spins ($S \neq S'$). (b) $\Sigma_{11}^{1/2}$ vs m' with $m = 10$ and $S = S' = 0$ and $S = 5, S' = m'/2$. The dashed lines in (a) are the dense limit results. See text for details.

Using these in Eq. (6.4.6), with $\lambda_0 = \lambda_1 = \lambda$, we have

$$\overline{\sigma_H^2(m, S)} = \lambda^2 \frac{\left(m^2 + 4\mathscr{S}^2\right)^2}{16}$$

(6.4.10)

$$\Rightarrow \left[\overline{\sigma_H^2(m, S_{max})}\right]^{-1} \overline{\sigma_H^2(m, S)} = \left[\frac{m/(m+2) + \mathscr{S}^2/\mathscr{S}_{max}^2}{m/(m+2) + 1}\right]^2.$$

The dense limit result given by Eq. (6.4.10) with $m = 2000$ is compared with the exact results in Fig. 6.5. Firstly, it should be noted that for the applicability of Eq. (6.4.10), Ω should be sufficiently large and $m \gg \Omega$. Also, the result is independent of Ω. Com-

176

paring with the $\Omega = 12$ and $\Omega = 40$ results, it is seen that the dense limit result is very close to the $\Omega = 40$ results for $m \gtrsim 200$. Thus for sufficiently large value of Ω and $m \gtrsim 5\Omega$, the dense limit result describes quite well the exact results.

Simplifying $\overline{\langle H \rangle^{m,S} \langle H \rangle^{m',S'}}$ gives in the dilute limit,

$$\overline{\langle H \rangle^{m,S} \langle H \rangle^{m',S'}}$$

(6.4.11)

$$= \frac{\lambda^2}{16\Omega^2} \left[\left(m^2 - 4\mathscr{S}^2 \right) \left\{ (m')^2 - 4(\mathscr{S}')^2 \right\} + \left(3m^2 + 4\mathscr{S}^2 \right) \left\{ 3(m')^2 + 4(\mathscr{S}')^2 \right\} \right] .$$

Then $[\Sigma_{11}]^{1/2}$, with $m = m'$ and $S = S'$ (for $\lambda_0 = \lambda_1$) giving ΔE_c, is

$$[\Sigma_{11}]^{1/2} = \Delta E_c = \frac{\sqrt{2(5m^4 + 8m^2\mathscr{S}^2 + 16(\mathscr{S}^2)^2)}}{\Omega \left(m^2 + 4\mathscr{S}^2 \right)} .$$

(6.4.12)

Eq. (6.4.12) gives $[\Sigma_{11}]^{1/2}$ to be $\sqrt{10}/\Omega$ and $2/\Omega$ for $S = 0$ and $S = S_{max}$ and these dense limit results are well verified by the results in Fig. 6.6(b). Similarly, Eqs. (6.4.10) and (6.4.11) will give $[\Sigma_{11}]^{1/2}$ to be $\sqrt{6}/\Omega$ for $(m = m' : S = S_{max}, S' = 0)$ and $2/\Omega$ for $(m = m' : S = S_{max}, S' = S_{max} - 1)$. The upper and lower dashed lines in Fig. 6.7(a) for $\Omega = 12$ (similarly for $\Omega = 40$) correspond to these two dense limit results, respectively. It is seen that the dense limit results are close to exact results for $\Omega = 40$ but there are deviations for $\Omega = 12$. Also, for $\Omega = 40$, the agreements are good only for $m \gtrsim 80$ and these are similar to the results discussed earlier with reference to Fig. 6.5.

Unlike for the covariances in energy centroids, we do not have at present complete analytical formulation for the covariances in spectral variances. However, for a given member of BEGOE(2)-s, generating numerically (on a computer) the ensembles $\{V^{s=0}(2)\}$ and $\{V^{s=1}(2)\}$ and applying Eqs. (6.4.1) and (6.4.2) to each member of the ensemble will give $\overline{\langle H^2 \rangle^{m,S}} = \overline{\sigma^2(m, S)} + \overline{[E_c(m, S)]^2}$. This procedure has been used with 500 members and results for Σ_{22} are obtained for various (Ω, m, S) values. For some examples, results are shown in Fig. 6.8 for both self-correlations giving the width $\Delta \langle H^2 \rangle^{m,S}$ of variances and cross-correlations $[\Sigma_{22}]^{1/2}$ with $(m, S) \neq (m', S')$. It is seen that $[\Sigma_{22}]^{1/2}$ are always much smaller than $[\Sigma_{11}]^{1/2}$ just as for EGOE(2) for spinless fermion systems [Ko-06a]. It is seen from Fig. 6.8(a) that for $\Omega = 12$, width of the fluctuations in the variances $\langle H^2 \rangle^{m,S}$ are $\sim 3 - 5\%$. Similarly for large m, with Ω very
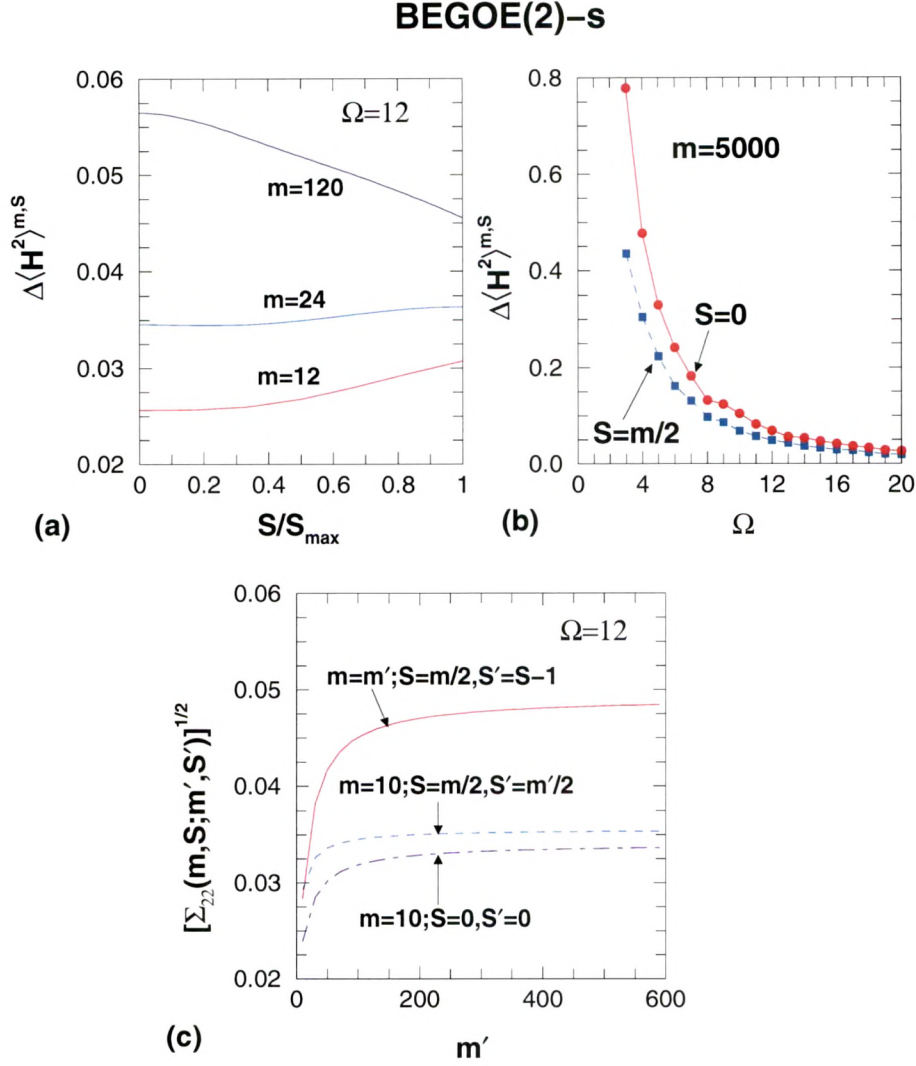
177

BEGOE(2)–s

Figure 6.8: Correlations in spectral variances $\Sigma_{22}^{1/2}$ for various BEGOE(2)-**s** systems. (a) Self-correlations, giving width $\Delta\langle H^2\rangle^{m,S}$ of the spectral variances, as a function of spin S for $m = 12, 24$ and 120 with $\Omega = 12$. (b) Self-correlations as a function of Ω for 5000 bosons with $S = 0$ and 2500. (c) Three examples for cross-correlation in spectral variances with same or different particle numbers and same or different spins. All the results are obtained using 500 member ensembles. See text for details.

small, the widths are quite large but they decrease fast with increasing Ω as seen from Fig. 6.8(b). Finally, for $\Omega = 12$, the cross-correlations are $\sim 4\%$. Finally, let us add that it is important to identify measures involving Σ_{11} and Σ_{22} that can be tested using some experiments so that evidence for BEGOE(2) operation in real quantum systems can be established.

6.5 Preponderance of $S_{max} = m/2$ Ground States and Natural Spin Order : Role of Exchange Interaction

6.5.1 Introduction to regular structures with random interactions

Johnson et al [Jo-98] discovered in 1998 that the nuclear shell-model with random interactions generates, with high probability, 0^+ ground states in even-even nuclei (also generates odd-even staggering in binding energies, the seniority pairing gap etc.) and similarly, Bijker and Frank [Bi-00] found that the interacting boson model (sdIBM) of atomic nuclei [in this model, one considers identical bosons carrying angular-momentum $\ell = 0$ (called s bosons) and $\ell = 2$ (called d bosons)] with random interactions generates vibrational and rotational structures with high probability. Starting with these, there are now many studies on regular structures in many-body systems generated by random interactions. See for example [Zh-04a,Ze-04,We-09] for reviews on the subject and Sec. 5.4.3 for results on preponderance of +ve parity ground states. More recently, the effect of random interactions in the pn-sdIBM with F-spin quantum number has been studied by Yoshida et al [Yo-09]. Here, proton and neutron bosons are treated as the two components of a spin $\frac{1}{2}$ boson and this spin is called F-spin. Yoshida et al found that random interactions conserving F-spin generate predominance of maximum F-spin (F_{max}) ground states. It should be noted that the low-lying states generated by pn-sdIBM correspond to those of sdIBM and all sdIBM states will have $F = F_{max}$. Thus random interactions preserve the property that the low-lying states generated by pn-sdIBM are those of sdIBM. Similarly, using shell-model with isospin conserving interactions (here protons and neutrons correspond to the two projections of isospin $t = \frac{1}{2}$), Kirson and Mizrahi [Ki-07] showed that random interactions generate natural isospin ordering. Denoting the lowest energy state (les) for a given many nucleon isospin T by $E_{les}(T)$, the natural isospin ordering corresponds to $E_{les}(T_{min}) \leq E_{les}(T_{min} + 1) \leq \ldots$; for even-even N=Z nuclei, $T_{min} = 0$. Therefore, one can ask if BEGOE(1+2)-**s** generates a spin ordering.

As an application of BEGOE(1+2)-**s**, we present here results for the probability of gs spin to be $S = S_{max}$ and also for natural spin ordering (NSO). Here NSO corresponds to $E_{les}(S_{max}) \leq E_{les}(S_{max} - 1)\ldots$. In this analysis, we add the Majorana force

or the space exchange operator to the Hamiltonian in Eq. (6.2.1). Note that S in BEGOE(1+2)-**s** is similar to F-spin in the pn-sdIBM. First we will derive the exchange interaction and then present some numerical results.

6.5.2 $U(\Omega)$ algebra and space exchange operator

In terms of boson creation $(b^\dagger)$ and annihilation (b) operators, the sp states for $(\Omega)^m$ systems are $\left| i, m_s \pm \frac{1}{2} \right\rangle = b^\dagger_{i,\frac{1}{2},m_s} |0\rangle$ with $i = 1, 2, \ldots, \Omega$. It can be easily identified that the $4\Omega^2$ number of one-body operators $A^r_{ij;\mu}$,

$$A^r_{ij;\mu} = \left(b^\dagger_i \tilde{b}_j \right)^r_\mu \; ; \quad r = 0, 1, \tag{6.5.1}$$

generate $U(2\Omega)$ algebra. In Eq. (6.5.1), $\tilde{b}_{i,\frac{1}{2},m_s} = (-1)^{\frac{1}{2}+m_s} b_{i,\frac{1}{2},-m_s}$. The $U(2\Omega)$ irreducible representations are denoted trivially by the particle number m as they must be symmetric irreps $\{m\}$. The Ω^2 number of operators A^0_{ij} generate $U(\Omega)$ algebra and similarly there is a $U(2)$ algebra generated by the number operator $\hat{n}$ and the spin generators S^1_μ,

$$\hat{n} = \sqrt{2} \sum_i A^0_{ii} \; ; \quad S^1_\mu = \frac{1}{\sqrt{2}} \sum_i A^1_{ii;\mu} \; . \tag{6.5.2}$$

Then we have the group-subgroup algebra $U(2\Omega) \supset U(\Omega) \otimes SU(2)$ with $SU(2)$ generated by S^1_μ. Note that $S_0 = S^1_0$, $S_+ = -\sqrt{2}S^1_1$ and $S_- = \sqrt{2}S^1_{-1}$. As the $U(2)$ irreps are two-rowed, the $U(\Omega)$ irreps have to be two-rowed and they are labeled by $\{m_1, m_2\}$ with $m = m_1 + m_2$ and $S = (m_1 - m_2)/2$; $m_1 \geq m_2 \geq 0$. Thus with respect to $U(\Omega) \otimes SU(2)$ algebra, many boson states are labeled by $|\{m_1, m_2\}, \xi\rangle$ or equivalently by $|(m, S), \xi\rangle$, where ξ are extra labels required for a complete specification of the states. The quadratic Casimir operator of the $U(\Omega)$ algebra is,

$$C_2[U(\Omega)] = 2 \sum_{i,j} A^0_{ij} \cdot A^0_{ji} \tag{6.5.3}$$

and its eigenvalues are $\langle C_2[U(\Omega)]\rangle^{\{m_1, m_2\}} = m_1(m_1 + \Omega - 1) + m_2(m_2 + \Omega - 3)$ or equivalently,

$$\langle C_2[U(\Omega)]\rangle^{(m,S)} = \frac{m}{2}(2\Omega + m - 4) + 2S(S + 1) \; . \tag{6.5.4}$$

Note that the Casimir invariant of $SU(2)$ is $\hat{S}^2$ with eigenvalues $S(S+1)$. Now we will show that the space exchange or the Majorana operator $\widehat{M}$ is simply related to $C_2[U(\Omega)]$.

Majorana operator $\widehat{M}$ acting on a two-particle state exchanges the spatial coordinates of the particles (index i) and leaves the spin quantum numbers (m_s) unchanged. The operator form of $\widehat{M}$ is

$$\widehat{M} = \frac{\kappa}{2} \sum_{i,j,m_s,m_s'} \left(b_{j,m_s}^\dagger b_{i,m_s'}^\dagger \right) \left(b_{i,m_s}^\dagger b_{j,m_s'}^\dagger \right)^\dagger . \tag{6.5.5}$$

Equation (6.5.5) gives, with κ a constant,

$$\widehat{M} = \frac{\kappa}{2} \{C_2[U(\Omega)] - \Omega\hat{n}\} . \tag{6.5.6}$$

Then, combining Eqs. (6.5.4) and (6.5.6), we have

$$\widehat{M} = \kappa \left\{ \hat{n}\left(\frac{\hat{n}}{4} - 1\right) + \hat{S}^2 \right\} . \tag{6.5.7}$$

As seen from Eq. (6.5.7), exchange interaction with $\kappa > 0$ generates gs with $S = S_{min} = 0(\frac{1}{2})$ for even(odd) m (this is opposite to the result for 'fermion systems' where the exchange interaction generates gs with $S = S_{max} = m/2$ [Ma-10, Ja-01]). Now we will study the interplay between random interactions and the Majorana force in generating gs spin structure in boson systems. Note that for states with boson number fixed, $\widehat{M} \propto \hat{S}^2$ as seen from Eq. (6.5.7) and therefore, from now on, we refer to $\hat{S}^2$ as the exchange interaction just as in Chapter 3.

6.5.3 Numerical results for $S_{max} = m/2$ ground states and natural spin order

In order to understand the gs structure in BEGOE(1+2)-s, we have studied $P(S = S_{max})$, the probability for the gs to be with spin $S_{max} = m/2$, by adding the exchange term $\lambda_S S^2$ with $\lambda_S > 0$ to the Hamiltonian in Eq. (6.2.1) i.e., using

$$\{H\}_{\text{BEGOE(1+2)-s:Exch}} = h(1) + \lambda \left[\{V^{s=0}(2)\} + \{V^{s=1}(2)\} \right] + \lambda_S S^2 . \tag{6.5.8}$$

181

BEGOE(1+2)–s:Exch

$\Omega=4$, **m=10**

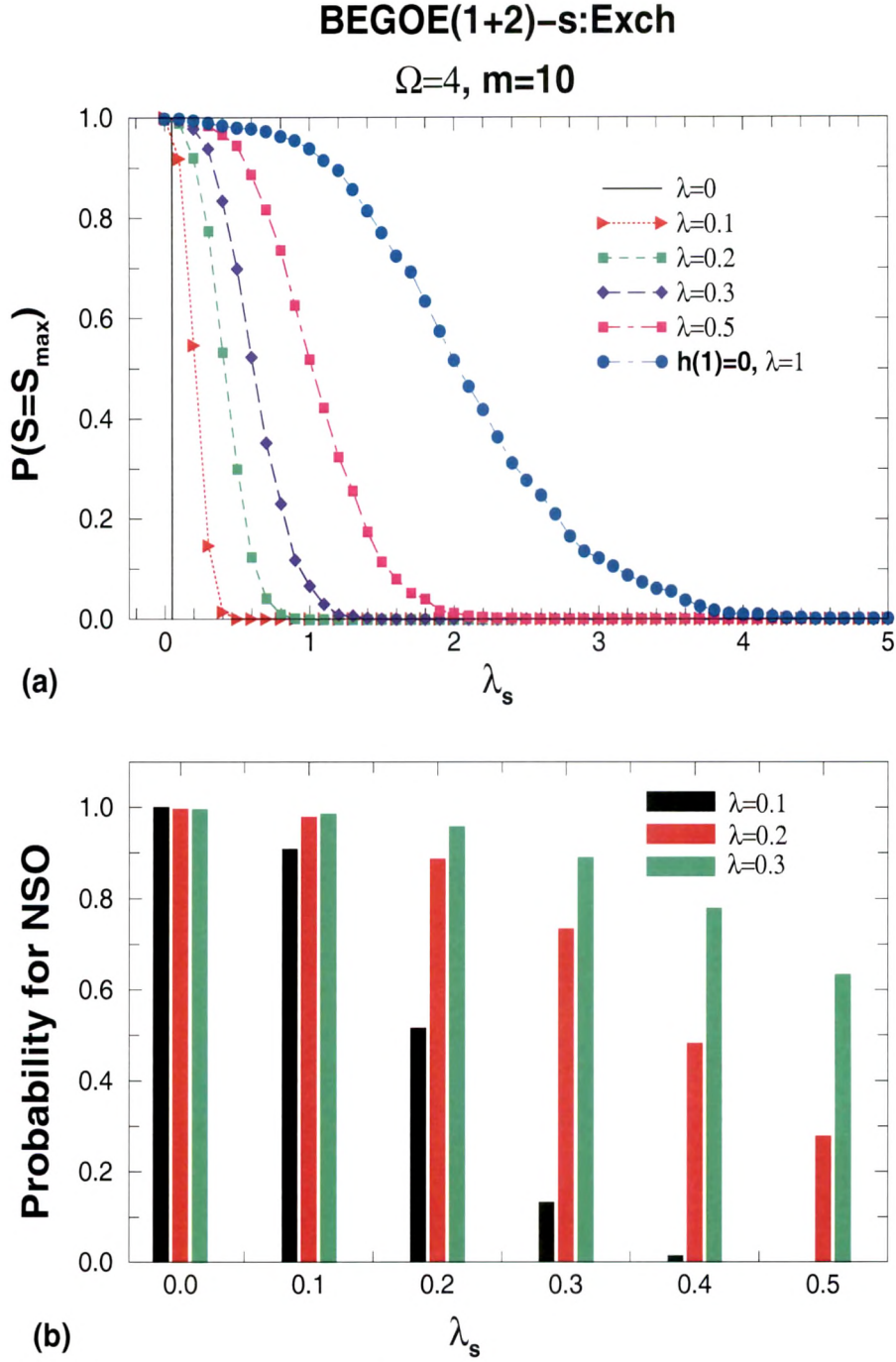**Figure 6.9:** (a) Probability for ground states to have spin $S = S_{max}$ as a function of the exchange interaction strength $\lambda_S \geq 0$. (b) Probability for natural spin order (NSO) as a function of λ_S. Results are shown for a 500 member BEGOE(1+2)-**s** : Exch ensemble generated by Eq. (6.5.8) for a system with $\Omega = 4$ and $m = 10$. Values of the interaction strength λ are shown in the figure.

Note that the operator S^2 is simple in the (m, S) basis. Fig. 6.9(a) gives probability $P(S = S_{max})$ for the ground states to have spin $S = S_{max}$ as a function of exchange interaction strength λ_S for $\lambda_0 = \lambda_1 = \lambda = 0$, 0.1, 0.2, 0.3 and 0.5 and also for $h(1) = 0$ with $\lambda = 1$. Similarly, Fig. 6.9(b) shows the results for NSO. Calculations are carried out for $(\Omega = 4$, $m = 10)$ system using a 500 member ensemble and the mean-field Hamiltonian $h(1)$ is as defined in Sec. 6.2.

Preponderance of $S_{max} = m/2$ ground states

Let us begin with pure random two-body interactions. Then $h(1) = 0$ in Eq. (6.5.8). Now in the absence of the exchange interaction $(\lambda_S = 0)$, as seen from Fig. 6.9(a), ground states will have $S = S_{max}$ i.e., the probability $P(S = S_{max}) = 1$. The variance propagator (see Fig. 6.5) derived earlier gives a simple explanation for this by applying the Jacquod and Stone prescription given by Eq. (4.6.1) with f_m replaced by S for BEGOE(1+2)-s. Thus pure random interactions generate preponderance of $S = S_{max}$ ground states. On the other hand, as discussed in Sec. 6.5.2, the exchange interaction acts in opposite direction by generating $S = S_{min}$ ground states. Therefore, by adding the exchange interaction to the $\{V(2)\}$ ensemble, $P(S = S_{max})$ starts decreasing as the strength λ_S $(\lambda_S > 0)$ starts increasing. For the example considered in Fig. 6.9(a), for $\lambda_S > 4$, we have $P(S = S_{max}) \sim 0$. The complete variation with λ_S is shown in Fig. 6.9(a) marked $h(1) = 0$ and $\lambda = 1$.

Similarly, on the other end, for $\lambda = 0$ in Eq. (6.5.8), we have $H = h(1)$ in the absence of the exchange interaction. In this situation, as all the bosons can occupy the lowest sp state, gs spin $S = S_{max}$. Therefore, $P(S = S_{max}) = 1$. When the exchange interaction is turned on, $P(S = S_{max})$ remains unity until λ_S equals the spacing between the lowest two sp states divided by m. As in our example, the sp energies are $\epsilon_i = i + 1/i$, we have $P(S = S_{max}) = 1$ for $\lambda_S < 0.05$. Then $P(S = S_{max})$ drops to zero for $\lambda_S \geq 0.05$. This variation with λ_S is shown in Fig. 6.9(a) marked $\lambda = 0$. Figure 6.9(a) also shows the variation of $P(S = S_{max})$ with λ_S for several values of λ between 0.1 and 0.5. It is seen that there is a critical value (λ_S^c) of λ_S after which $P(S = S_{max}) = 0$ and its value increases with λ. Also, the variation of $P(S = S_{max})$ with λ_S becomes slower as λ increases.

In summary, results in Fig. 6.9(a) clearly show that with random interactions there

183

is preponderance of $S = S_{max} = m/2$ ground states. This is unlike for fermions where there is preponderance of $S = S_{min} = 0(\frac{1}{2})$ ground states for m even(odd); see Fig. 3.5. With the addition of the exchange interaction, $P(S = S_{max})$ decreases and finally goes to zero for $\lambda_S \geq \lambda_S^c$ and the value of λ_S^c increases with λ. We have also carried out calculations for $(\Omega = 4, m = 11)$ system using a 100 member ensemble and the results are close to those given in Fig. 6.9(a). All these explain the results given in [Yo-09] where random interactions are employed within pn-sdIBM.

Natural spin ordering

For the system considered in Fig. 6.9(a), for each member of the ensemble, eigenvalue of the lowest state for each spin S is calculated and using these, we have obtained total number of members N_λ having NSO as a function of λ_S for $\lambda = 0.1, 0.2$ and 0.3 using the Hamiltonian given in Eq. (6.5.8). As stated in Sec. 6.5.1, the NSO here corresponds to (as $S = S_{max}$ is the spin of the gs of the system) $E_{les}(S_{max}) <$ $E_{les}(S_{max}-1) < E_{les}(S_{max}-2) < \ldots$. The probability for NSO is $N_\lambda/500$ and the results are shown in Fig. 6.9(b). In the absence of the exchange interaction, as seen from Fig. 6.9(b), NSO is found in all the members independent of λ. Thus random interactions strongly favor NSO. The presence of exchange interaction reduces the probability for NSO. Comparing Figs. 6.9(a) and (b), it is clearly seen that with increasing exchange interaction strength, probability for gs state spin to be $S = S_{max}$ is preserved for much larger values of λ_S (with a fixed λ) compared to the NSO. Therefore for preserving both $S = S_{max}$ gs and the NSO with high probability, the λ_S value has to be small. We have also verified this for the $(\Omega = 4, m = 11)$ system. Finally, it is plausible to argue that the results in Fig. 6.9 obtained using BEGOE(1+2)-s are generic for boson systems with spin. Now we will turn to pairing in BEGOE(2)-s.

6.6 Pairing in BEGOE(2)-s

Pairing correlations are known to be important not only for fermion systems (see Chapter 3) but also for boson systems [Pe-10]. An important issue that is raised in the recent years is: to what extent random interactions carry features of pairing. See Chapter 3 and [Zh-04a, Ze-04, Ho-07] for some results for fermion systems. In order to address this question for boson systems, first we will identify the pairing algebra in

(Ω, m, S) spaces of BEGOE(2)-**s**. Then we will consider expectation values of the pairing Hamiltonian in the eigenstates generated by BEGOE(2)-**s** as they carry signatures of pairing.

6.6.1 $U(2\Omega) \supset [U(\Omega) \supset SO(\Omega)] \otimes SU_S(2)$ **Pairing symmetry**

In constructing BEGOE(2)-**s**, it is assumed that spin is a good symmetry and thus the m-particle states carry spin (S) quantum number. Now, following the $SO(5)$ pairing algebra for fermions [Fl-64], it is possible to consider pairs that are vectors in spin space. The pair creation operators $P_{i:\mu}$ for the level i and the generalized pair creation operators (over the Ω levels) P_μ, with $\mu = -1, 0, 1$, in spin coupled representation, are

$$P_\mu = \frac{1}{\sqrt{2}} \sum_i \left(b_i^\dagger b_i^\dagger \right)^1_\mu = \sum_i P_{i:\mu}, \quad \left(P_\mu \right)^\dagger = \frac{1}{\sqrt{2}} \sum_i (-1)^{1-\mu} \left(\tilde{b}_i \tilde{b}_i \right)^1_{-\mu}. \tag{6.6.1}$$

Therefore in the space defining BEGOE(2)-s, the pairing Hamiltonian H_p and its two-particle matrix elements are,

$$H_p = \sum_\mu P_\mu \left(P_\mu \right)^\dagger, \quad \langle (k\ell)s \mid H_p \mid (ij)s \rangle = \delta_{s,1} \delta_{i,j} \delta_{k,\ell}. \tag{6.6.2}$$

With this, we will proceed to identify and analyze the pairing algebra. It is easy to verify that the $\Omega(\Omega - 1)/2$ number of operators $C_{ij} = A^0_{ij} - A^0_{ji}$, $i > j$ generate a $SO(\Omega)$ subalgebra of the $U(\Omega)$ algebra; $A^r_{ij:\mu}$ are defined in Eq. (6.5.1). Therefore we have $U(2\Omega) \supset [U(\Omega) \supset SO(\Omega)] \otimes SU(2)$. We will show that the irreps of $SO(\Omega)$ algebra are uniquely labeled by the seniority quantum number v and a reduced spin $\tilde{s}$ similar to the reduced isospin introduced in the context of nuclear shell-model [Fl-52] and they in turn define the eigenvalues of H_p. The quadratic Casimir operator of the $SO(\Omega)$ algebra is,

$$C_2[SO(\Omega)] = 2 \sum_{i>j} C_{ij} \cdot C_{ji}. \tag{6.6.3}$$

Carrying out angular-momentum algebra [Ed-74] it can be shown that,

$$C_2[SO(\Omega)] = C_2[U(\Omega)] - 2 H_p - \hat{n}. \tag{6.6.4}$$

The quadratic Casimir operator of the $U(\Omega)$ algebra is given in Eq. (6.5.3). Before discussing the eigenvalues of the pairing Hamiltonian H_p, let us first consider the irreps of $SO(\Omega)$.

Given the two-rowed $U(\Omega)$ irreps $\{m_1, m_2\}$; $m_1 + m_2 = m$, $m_1 - m_2 = 2S$, it should be clear that the $SO(\Omega)$ irreps should be of $[\nu_1, \nu_2]$ type and for later simplicity we use $\nu_1 + \nu_2 = \nu$ and $\nu_1 - \nu_2 = 2\tilde{s}$. The quantum number ν is called seniority and $\tilde{s}$ is called reduced spin; see also Appendix D. The $SO(\Omega)$ irreps for a given $\{m_1, m_2\}$ can be obtained as follows. First expand the $U(\Omega)$ irrep $\{m_1, m_2\}$ in terms of totally symmetric irreps,

$$\{m_1, m_2\} = \{m_1\} \times \{m_2\} - \{m_1 + 1\} \times \{m_2 - 1\}. \tag{6.6.5}$$

Note that the irrep multiplication in Eq. (6.6.5) is a Kronecker multiplication [Ko-06c, Wy-70]. For a totally symmetric $U(\Omega)$ irrep $\{m'\}$, the $SO(\Omega)$ irreps are given by the well-known result

$$\{m'\} \rightarrow [\nu] = [m'] \oplus [m' - 2] \oplus \ldots \oplus [0] \text{ or } [1]. \tag{6.6.6}$$

Finally, reduction of the Kronecker product of two symmetric $SO(\Omega)$ irreps $[\nu_1]$ and $[\nu_2]$, $\Omega > 3$ into $SO(\Omega)$ irreps $[\nu_1, \nu_2]$ is given by (for $\nu_1 \geq \nu_2$) [Ko-06c, Wy-70],

$$[\nu_1] \times [\nu_2] = \sum_{k=0}^{\nu_2} \sum_{r=0}^{\nu_2 - k} [\nu_1 - \nu_2 + k + 2r, k] \oplus . \tag{6.6.7}$$

Combining Eqs. (6.6.5), (6.6.6) and (6.6.7) gives the $\{m_1, m_2\} \rightarrow [\nu_1, \nu_2]$ reductions. It is easy to implement this procedure on a computer.

Given the space defined by $|\{m_1, m_2\}, [\nu_1, \nu_2], \alpha\rangle$, with α denoting extra labels needed for a complete specification of the state, the eigenvalues of $C_2[SO(\Omega)]$ are [Ko-06c]

$$\langle C_2[SO(\Omega)]\rangle^{\{m_1, m_2\}, [\nu_1, \nu_2]} = \nu_1(\nu_1 + \Omega - 2) + \nu_2(\nu_2 + \Omega - 4). \tag{6.6.8}$$

Now changing $\{m_1, m_2\}$ to (m, S) and $[\nu_1, \nu_2]$ to $(\nu, \tilde{s})$ and using Eqs. (6.6.4) and (6.5.4) will give the formula for the eigenvalues of the pairing Hamiltonian H_p. The final

result is,

$$E_p(m, S, v, \tilde{s}) = \langle H_p \rangle^{m,S,v,\tilde{s}} = \frac{1}{4}(m - v)(2\Omega - 6 + m + v) + [S(S+1) - \tilde{s}(\tilde{s}+1)]. \quad (6.6.9)$$

This is same as the result that follows from Eq. (18) of [Fl-64] for fermions by using $\Omega \rightarrow -\Omega$ symmetry; see also Eq. (D4). From now on, we denote the $U(\Omega)$ irreps by (m, S) and $SO(\Omega)$ irreps by $(v, \tilde{s})$. In Table 6.1, for $(\Omega, m) = (4, 10), (5, 8)$ and $(6, 6)$ systems, given are the $(m, S) \rightarrow (v, \tilde{s})$ reductions, the pairing eigenvalues given by Eq. (6.6.9) in the spaces defined by these irreps and also the dimensions of the $U(\Omega)$ and $SO(\Omega)$ irreps. The dimensions $d_b(\Omega, m, S)$ of the $U(\Omega)$ irreps (m, S) are given by Eq. (6.2.2). Similarly, the dimension $d(v_1, v_2) \Leftrightarrow d(v, \tilde{s})$ of the $SO(\Omega)$ irreps $[v_1, v_2]$ follow from Eqs. (6.6.6) and (6.6.7) and they will give

$$d(v_1, v_2) = d(v_1)d(v_2) - \sum_{k=0}^{v_2-1} \sum_{r=0}^{v_2-k} d(v_1 - v_2 + k + 2r, k) \, ;$$

$$(6.6.10)$$

$$d(v) = \binom{\Omega + v - 1}{v} - \binom{\Omega + v - 3}{v - 2} .$$

Note that in general the $SO(\Omega)$ irreps $(v, \tilde{s})$ can appear more than once in the reduction of $U(\Omega)$ irreps (m, S). For example, $(2, 1)$ irrep of $SO(\Omega)$ appears twice in the reduction of the $U(\Omega)$ irrep $(10, 1)$.

It is useful to remark that just as the fermionic $SO(5)$ pairing algebra for nucleons in j orbits [Pa-65, He-65, Fl-64], there will be a $SO(4, 1)$ complementary pairing algebra corresponding to the $SO(\Omega)$ subalgebra. The ten operators P_μ^1, $(P_\mu^1)^\dagger$, S_μ^1 and $\hat{n}$ form the $SO(4, 1)$ algebra. Their commutation relations follow from the basic two commutation relations,

$$\left[P_{\mu_1}^1, \left(P_{\mu_2}^1 \right)^\dagger \right] = -\left(\Omega + \hat{n} + 2\mu S_0^1 \right) \text{ for } \mu_1 = \mu_2 = \mu$$

$$(6.6.11)$$

$$= 2\sqrt{2}(-1)^{\mu_2} \langle 1\mu_1 1 - \mu_2 \mid 1\mu_1 - \mu_2 \rangle S_{\mu_1-\mu_2}^1 \text{ for } \mu_1 \neq \mu_2 ,$$

$$\left[\sqrt{2} P_{\mu_1}^1, \left(b^\dagger \tilde{b} \right)_{\mu_2}^s \right] = \sqrt{6(2s+1)}(-1)^{s+1} \left\langle 1\mu_1 s\mu_2 \mid 1\mu_1 + \mu_2 \right\rangle$$

$$\times \left\{ \begin{matrix} 1 & \frac{1}{2} & \frac{1}{2} \\ \frac{1}{2} & 1 & s \end{matrix} \right\} P_{\mu_1 + \mu_2}^1 ; \quad s = 0, 1.$$

It is possible, in principle, to exploit this algebra to derive properties of the eigenstates defined by the pairing Hamiltonian.

6.6.2 Pairing expectation values

Pairing expectation values are defined by $\left\langle H_p \right\rangle^{S,E} = \left\langle m, S, E \mid H_p \mid m, S, E \right\rangle$ for eigenstates with energy E and spin S generated by a Hamiltonian H for a system of m bosons in Ω number of sp orbitals (for simplicity, we have dropped Ω and m labels in $\left\langle H_p \right\rangle^{S,E}$). In our analysis, H is a member of BEGOE(2)-s. As we will be comparing the results for all spins at a given energy E, for each member of the ensemble the eigenvalues for all spins are zero centered and normalized using the m-particle energy centroid $E_c(m) = \langle H \rangle^m$ and spectrum width $\sigma(m) = [\langle H^2 \rangle^m - \{E_c(m)\}^2]^{1/2}$. Then the eigenvalues E for all S are changed to $\widehat{E} = [E - E_c(m)]/\sigma(m)$. Using the method described in Sec. 6.2, the H_p matrix is constructed in good M_S basis and transformed into the eigenbasis of a given S for each member of the BEGOE(2)-s ensemble. Then the ensemble average of the diagonal elements of the H_p matrix will give the ensemble averaged pairing expectation values $\overline{\left\langle H_p \right\rangle^{S,E}} \Leftrightarrow \overline{\left\langle H_p \right\rangle^{S,\widehat{E}}}$. Using this procedure for a 500 member BEGOE(2)-s ensemble with $\Omega = 4$, $m = 10$ and $S = 0 - 5$, results for $\left\langle H_p \right\rangle^{S,\widehat{E}}$ as a function of energy $\widehat{E}$ (with $\widehat{E}$ as described above) and spin S are obtained and they are shown as a 3D histogram in Fig. 6.10. From Table 6.1, it is seen that the maximum value of the eigenvalues $E_p(m, S, v, \tilde{s})$ increases with spin S for a fixed-(Ω, m). The values are 28, 32, 34, 42, 48, and 60 for $S = 0 - 5$, respectively for $\Omega = 4$ and $m = 10$. Numerical results in Fig. 6.10 also show that for states near the lowest $\widehat{E}$ value, $\left\langle H_p \right\rangle^{S,\widehat{E}}$ increases with spin S. Thus random interactions preserve this property of the pairing Hamiltonian in addition to generating $S = S_{max}$ ground states as discussed in Sec. 6.5.3. It is useful to remark that random interactions will not generate $S = S_{max}$ ground states with $(v, \tilde{s}) = (m, m/2)$ as required for example in the pn-sdIBM. This needs explicit inclusion of pairing and exchange terms in the

Hamiltonians defined by Eqs. (6.2.1) and (6.3.1).

Table 6.1: Classification of states in the $U(2\Omega) \supset [U(\Omega) \supset SO(\Omega)] \otimes SU_S(2)$ limit for $(\Omega, m) = (4,10),(5,8)$ and $(6,6)$. Given are $U(\Omega)$ labels (m,S) and $SO(\Omega)$ labels $(v,\tilde{s})$ with the corresponding dimensions $d_b(\Omega,m,S)$ and $d(v,\tilde{s})$, respectively, and also the pairing eigenvalues $E_p = E_p(m,S,v,\tilde{s})$. Note that $\sum_{v,\tilde{s}} r\,d(v,\tilde{s}) = d_b(\Omega,m,S)$; here r denotes multiplicity of the $SO(\Omega)$ irreps and in the table, they are shown only for the cases when $r > 1$.

Ω	m	$(m,S)_{d_b(\Omega,m,S)}$	$(v,\tilde{s})^r_{d(v,\tilde{s})}$	E_p	Ω	m	$(m,S)_{d_b(\Omega,m,S)}$	$(v,\tilde{s})^r_{d(v,\tilde{s})}$	E_p
4	10	$(10,0)_{196}$	$(2,0)_6$	28	5	8	$(8,0)_{490}$	$(0,0)_1$	24
			$(4,1)_{30}$	22				$(2,1)_{14}$	19
			$(6,2)_{70}$	12				$(4,2)_{55}$	10
			$(6,0)_{14}$	18				$(4,0)_{35}$	16
			$(8,1)_{54}$	8				$(6,1)_{220}$	7
			$(10,0)_{22}$	0				$(8,0)_{165}$	0
		$(10,1)_{540}$	$(2,1)^2_9$	28			$(8,1)_{1260}$	$(2,1)_{14}$	21
			$(4,2)^2_{25}$	20				$(4,2)_{55}$	12
			$(6,3)_{49}$	8				$(4,1)^2_{81}$	16
			$(4,1)_{30}$	24				$(6,2)_{260}$	5
			$(6,2)_{70}$	14				$(6,1)_{220}$	9
			$(6,1)^2_{42}$	18				$(8,1)_{455}$	0
			$(8,2)_{90}$	6				$(2,0)_{10}$	23
			$(8,1)_{54}$	10				$(6,0)_{84}$	11
			$(10,1)_{66}$	0			$(8,2)_{1500}$	$(4,2)^2_{55}$	16
			$(0,0)_1$	32				$(6,3)_{140}$	3
			$(4,0)_{10}$	26				$(6,2)_{260}$	9
			$(8,0)_{18}$	12				$(8,2)_{625}$	0
		$(10,2)_{750}$	$(4,2)^2_{25}$	24				$(2,1)^2_{14}$	25
			$(6,3)_{49}$	12				$(4,1)_{81}$	20
			$(6,2)^2_{70}$	18				$(6,1)_{220}$	13
			$(8,3)_{126}$	4				$(0,0)_1$	30
			$(8,2)_{90}$	10				$(4,0)_{35}$	22

Table 6.1 – continued

Ω	m	$(m,S)_{d_b(\Omega,m,S)}$	$(v,\bar{s})^r_{d(v,\bar{s})}$	E_p	Ω	m	$(m,S)_{d_b(\Omega,m,S)}$	$(v,\bar{s})^r_{d(v,\bar{s})}$	E_p
			$(10,2)_{110}$	0			$(8,3)_{1155}$	$(6,3)_{140}$	9
			$(2,1)_9$	32				$(8,3)_{595}$	0
			$(4,1)^2_{30}$	28				$(4,2)_{55}$	22
			$(6,1)_{42}$	22				$(6,2)_{260}$	15
			$(8,1)_{54}$	14				$(2,1)_{14}$	31
			$(2,0)_6$	34				$(4,1)_{81}$	26
			$(6,0)_{14}$	24				$(2,0)_{10}$	33
		$(10,3)_{770}$	$(6,3)^2_{49}$	18			$(8,4)_{495}$	$(8,4)_{285}$	0
			$(8,4)_{81}$	2				$(6,3)_{140}$	17
			$(8,3)_{126}$	10				$(4,2)_{55}$	30
			$(10,3)_{154}$	0				$(2,1)_{14}$	39
			$(4,2)^2_{25}$	30				$(0,0)_1$	44
			$(6,2)_{70}$	24	6	6	$(6,0)_{490}$	$(2,0)_{15}$	14
			$(8,2)_{90}$	16				$(4,1)_{175}$	6
			$(2,1)^2_9$	38				$(6,0)_{300}$	0
			$(4,1)_{30}$	34			$(6,1)_{1134}$	$(2,1)^2_{20}$	14
			$(6,1)_{42}$	28				$(4,2)_{105}$	4
			$(0,0)_1$	42				$(4,1)_{175}$	8
			$(4,0)_{10}$	36				$(6,1)_{729}$	0
		$(10,4)_{594}$	$(8,4)_{81}$	10				$(0,0)_1$	20
			$(10,4)_{198}$	0				$(4,0)_{84}$	10
			$(6,3)_{49}$	26			$(6,2)_{1050}$	$(4,2)_{105}$	8
			$(8,3)_{126}$	18				$(6,2)_{735}$	0
			$(4,2)_{25}$	38				$(2,1)_{20}$	18
			$(6,2)_{70}$	32				$(4,1)_{175}$	12
			$(2,1)_9$	46				$(2,0)_{15}$	20
			$(4,1)_{30}$	42			$(6,3)_{462}$	$(6,3)_{336}$	0
			$(2,0)_6$	48				$(4,2)_{105}$	14
		$(10,5)_{286}$	$(10,5)_{121}$	0				$(2,1)_{20}$	24

Table 6.1 – continued

Ω	m	$(m,S)_{d_b(\Omega,m,S)}$	$(v,\bar{s})^r_{d_{(v,\bar{s})}}$	E_p	Ω	m	$(m,S)_{d_b(\Omega,m,S)}$	$(v,\bar{s})^r_{d_{(v,\bar{s})}}$	E_p
			$(8,4)_{81}$	20				$(0,0)_1$	30
			$(6,3)_{49}$	36					
			$(4,2)_{25}$	48					
			$(2,1)_9$	56					
			$(0,0)_1$	60					

For a given spin S, the pairing expectation values as a function of E are expected, for two-body ensembles, to be given by a ratio of expectation value density Gaussian (the first two moments given by $\langle H_p H \rangle^{m,S}$ and $\langle H_p H^2 \rangle^{m,S}$) and the eigenvalue density Gaussian with normalization given by $\langle H_p \rangle^{m,S}$ and this itself will be a Gaussian; see Chapters 2 and 3 for details. Let us denote the expectation value density centroid by $E_c(m,S:H_p)$ and width by $\sigma(m,S:H_p)$. Then the ratio of Gaussians [see Eq. (3.4.2)] will give

$$\overline{\langle H_p \rangle}^{S,\widehat{E}} = \frac{\langle H_p \rangle^{m,S}}{\widehat{\sigma}(m,S)} \exp \frac{\widehat{\epsilon}^2(m,S)}{2\left[1-\widehat{\sigma}^2(m,S)\right]}$$

$$\times \exp\left\{ \frac{(\widehat{\sigma}^2(m,S)-1)}{2\widehat{\sigma}^2(m,S)} \left[\widehat{E} - \frac{\widehat{\epsilon}(m,S)}{1-\widehat{\sigma}^2(m,S)}\right]^2 \right\}.$$

(6.6.12)

Here, $\widehat{\epsilon}(m,S) = \{E_c(m,S:H_p) - E_c(m,S)\}/\sigma(m,S)$, $\widehat{\sigma}(m,S) = \sigma(m,S:H_p)/\sigma(m,S)$ and $\widehat{E} = [\sigma(m)/\sigma(m,S)]\{\widehat{E} - \mathscr{E}\}$; $\mathscr{E} = [E_c(m,S) - E_c(m)]/\sigma(m)$. The Gaussian form given by Eq. (6.6.12) is clearly seen in Fig. 6.10 and this also gives a quantitative description of the results. Note that in our example, $\widehat{\epsilon}(10,S) = 0.001, 0.001, 0.001, 0.002, 0.002, 0.003$ and $\widehat{\sigma}(10,S) = 1.045, 1.047, 1.053, 1.062, 1.073, 1.082$, respectively for $S = 0 - 5$.

6.7 Summary

In the present chapter, we have introduced the BEGOE(1+2)-s ensemble and a method for constructing BEGOE(1+2)-s for numerical calculations has been described. Numerical examples are used to show that, like the spinless BEGOE(1+2), the spin BEGOE(1+2)-s ensemble also generates Gaussian density of states in the
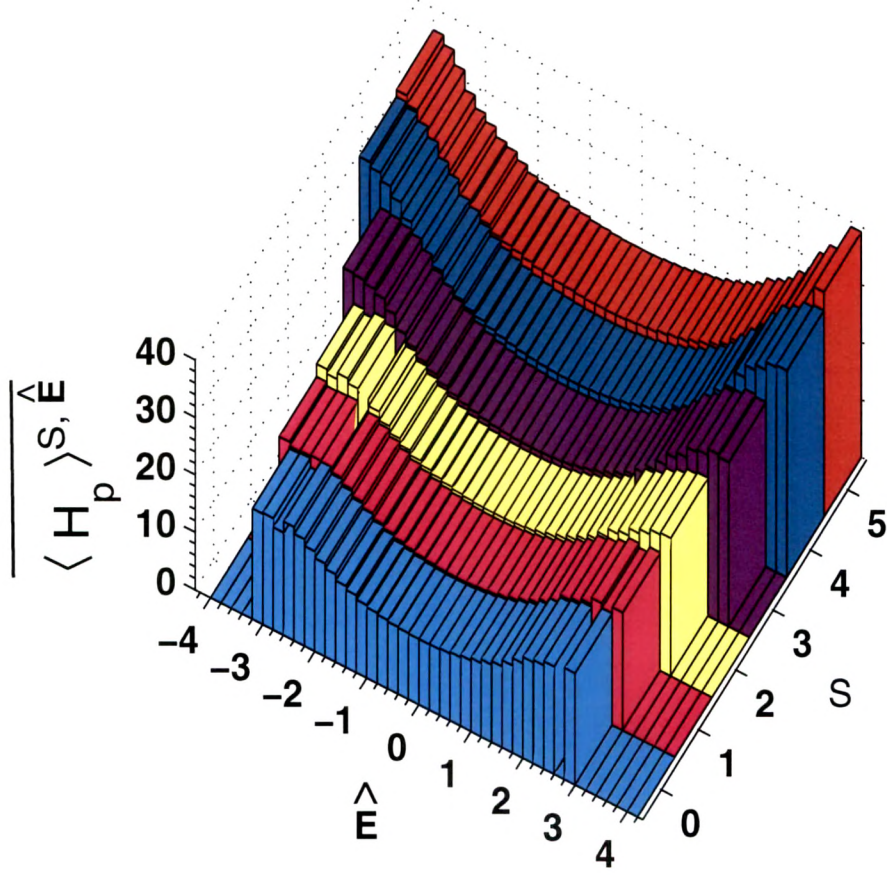
Figure 6.10: Ensemble averaged pairing expectation values $\overline{\langle H_p \rangle}^{S,\widehat{E}}$ vs $\widehat{E}$ and S, shown as a 3D histogram, for a 500 member BEGOE(2)-**s** ensemble with $\Omega = 4$ and $m = 10$. The bin-size is 0.2 for $\widehat{E}$. Note that the $\widehat{E}$ label in this figure is different from the $\widehat{E}$ used in Figs. 6.1 and 6.3(a).

dense limit. Similarly, BEGOE(2)-**s** exhibits GOE level fluctuations. On the other hand, BEGOE(1+2)-**s** exhibits Poisson to GOE transition as the interaction strength λ is increased and the transition marker λ_c is found to decrease with increasing spin. Moreover, ensemble averaged covariances in energy centroids and spectral variances for BEGOE(2)-**s** between spectra with different particle numbers and spins are studied using the propagation formulas derived for the energy centroids and spectral variances. For $\Omega = 12$ systems, the cross-correlations in energy centroids are $\sim 15\%$ and they reduce to $\sim 4\%$ for spectral variances. We have also derived the exact formula for the ensemble averaged fixed-(m, S) spectral variances and demonstrated

that the variance propagator gives a simple explanation for the preponderance of spin $S = S_{max}$ ground states generated by random interactions as in pn-sdIBM. It is also shown, by including exchange interaction $\hat{S}^2$ in BEGOE(1+2)-**s**, that random interactions preserving spin symmetry strongly favor NSO (just as with isospin in nuclear shell-model). These results are comprehensive and give a mathematical foundation for the results in [Yo-09]. In addition, we have identified the pairing $SO(\Omega)$ symmetry and showed using numerical examples that random interactions exhibit pairing correlations in the gs region and also they generate a Gaussian form for the variation of the pairing expectation values with respect to energy.